geosciences

MDPI

Review

Review of Hydraulic Fracture Diagnostics: Technologies, Interpretation Challenges, and Emerging Advances

Tianhao Bai *, Guan Qin and Mohamed Y. Soliman *

Department of Petroleum Engineering, Cullen College of Engineering, University of Houston, Houston, TX 77204, USA; gqin2@central.uh.edu

* Correspondence: tbai5@cougarnet.uh.edu (T.B.); msoliman@central.uh.edu (M.Y.S.)

Abstract

Hydraulic fracture diagnostics are essential for characterizing fracture geometry, connectivity, and effectiveness in unconventional reservoirs. However, the diversity of available techniques and fragmented understanding of their physical mechanisms hinder multidisciplinary communication and lead to inconsistent field decisions. This review provides a systematic assessment of diagnostic methods, focusing on their physical foundations, applicability, and limitations, and proposes a unified reference framework. Direct diagnostics, including microseismic monitoring, fiber-optic sensing (DTS and DAS), and tiltmeter measurements, are evaluated in terms of data characteristics, interpretation challenges, and field applicability. Indirect methods based on pressure, production, and tracer data—such as DFITs, pressure interference tests, and tracer analysis—are examined for their roles in fracture closure evaluation and interwell connectivity. The review further distinguishes between single-well and multi-well applications, providing a structured classification framework. It highlights that individual methods are constrained by non-uniqueness, modeling assumptions, and non-ideal field conditions, especially in complex fracture networks. Therefore, reliable characterization requires integrating multiple diagnostics with physics-based modeling and uncertainty-aware interpretation. Recent advances in AI and machine learning are also briefly discussed as tools to enhance automated analysis and support real-time, predictive diagnostics.

Keywords: fracture diagnostic technology; unconventional reservoir; hydraulic fracturing

1. Introduction

Hydrocarbon extraction from unconventional reservoirs accounts for a major share of the energy supply in the United States and relies heavily on advances in hydraulic fracturing and horizontal drilling. These technologies generate complex fracture systems that serve as primary flow pathways and enable economic production. In recent years, hydraulic fracturing approaches, including simultaneous fracturing, multi-fracture network development, stage fracturing, and refracturing—have further enhanced recovery and continuously improved project profitability [1–3].

Despite these advances, field statistics indicate that a substantial proportion of perforated fractures in shale formations do not contribute to production, underscoring the importance of effective fracture monitoring and evaluation [4]. Moreover, the lack of accurate prediction of fracture growth during the stimulation and production periods has led to operational challenges, such as unintended fluid leakage into non-productive zones or faults and incomplete recovery of flowback water, raising both economic and

Check for updates

Academic Editors: Yangkang Chen and Eun Young Lee

Received: 4 April 2026
Revised: 27 May 2026
Accepted: 3 June 2026
Published: 9 June 2026

Copyright: © 2026 by the authors. Licensee MDPI, Basel, Switzerland. This article is an open access article distributed under the terms and conditions of the Creative Commons Attribution (CC BY) license.

environmental concerns [5]. One contributing factor is the absence of consensus regarding the dominant physical mechanisms governing fracture initiation and propagation, as well as inconsistencies in the application of fracture diagnostic methodologies. Consequently, the theoretical foundations and computational models used in fracture growth simulation and performance evaluation remain uncertain.

Hydraulic fracturing operations inherently require close collaboration among multidisciplinary teams throughout planning, execution, and post-treatment evaluation. However, differences in disciplinary background often lead to fragmented interpretations of fracture diagnostic results. Therefore, a comprehensive and mechanism-oriented overview of fracture diagnostic technologies is needed to provide a unified technical perspective and reduce miscommunication among geoscientists, reservoir engineers, and completion engineers. Such an overview is particularly valuable for industry practitioners and decision makers who must translate diagnostic insights into practical operational strategies and optimized development plans.

Previous studies have reviewed fracture diagnostic techniques in unconventional reservoirs. For example, Webster et al. [6] investigated the integration of microseismic monitoring (MSM) and distributed acoustic sensing (DAS) in multi-well applications. Mahmoud et al. [7] provided a systematic review of existing diagnostic tools and their technological advancements, comparing the advantages and limitations of individual methods, summarizing integration outcomes, and identifying future development directions. While these studies offer valuable summaries of available techniques and their applications, they primarily focus on tool-level comparisons and integration outcomes, and are largely directed toward readers with established technical backgrounds in specific diagnostic domains. Less emphasis has been placed on the underlying physical mechanisms, operational boundaries, and the practical selection logic that guides diagnostic deployment across different field conditions—knowledge that is critical for multidisciplinary teams navigating real-world fracturing decisions. Notably, pressure interference testing—an increasingly relevant diagnostic approach in multi-well unconventional development—has received limited systematic treatment in existing reviews.

Accordingly, this review aims to bridge this gap by providing an accessible, mechanism-oriented overview of hydraulic fracture diagnostic technologies intended for a broad audience of researchers, field engineers, and decision makers involved in hydraulic fracturing design, monitoring, and optimization. The primary objective is not to reproduce the mathematical rigor of method-specific literature, but rather to clarify the physical foundations, historical development, applicability conditions, and operational limitations of each diagnostic approach in a unified and practically oriented framework. This distinction in scope and intent differentiates the present work from existing technically focused reviews. A unified classification framework is proposed that distinguishes between direct and indirect fracture detection methods, with indirect techniques further classified into single-well and multi-well application modes to explicitly reflect their deployment strategies and practical use cases. A comparative summary of all reviewed methods is provided to facilitate technology selection across different operational contexts, serving as a structured reference for multidisciplinary teams who require diagnostic literacy rather than method-specific expertise.

2. Literature Review of Diagnostic Technologies

This literature review is organized into direct and indirect fracture diagnostic methods, distinguished by the type of measured response and the physical mechanism used to infer fracture behavior. Direct diagnostics capture fracture-induced physical signals (e.g., seismicity, deformation, temperature, and strain), whereas indirect methods infer fracture

characteristics from pressure, flow, or tracer responses at the well or interwell scale. Below is the summary table (Table 1) of hydraulic fracture diagnostics method reviewed in this study, organized by primary output, application scale, and operational limitation.

Table 1. Comparative summary of hydraulic fracture diagnostic methods.

Direct Diagnostic Methods	Primary Output	Application Scale	Primary Limitation
Microseismic Monitoring	Fracture event locations, SRV extent, source mechanisms	Wellbore- to field-scale (deployment-dependent)	Velocity model dependency; cannot distinguish propped from unpropped fractures; susceptible to background noise
Distributed Temperature Sensing	Fluid distribution, fracture entry points, near-wellbore flow profile	Wellbore-scale	Thermal inversion non-uniqueness; strong model dependency; insufficient for complex fracture networks alone
Distributed Acoustic Sensing	Fracture-induced strain field, perforation cluster efficiency, interwell communication	Wellbore- and interwell-scale	Limited directional sensitivity; fiber-formation coupling uncertainty; large data volume requirements
Tiltmeter	Fracture orientation, fracture volume, dominant deformation mode	Field-scale	Fracture size estimation ill-posed in far-field deployment; requires complementary constraints for geometry reconstruction
Indirect Diagnostic Methods			
Diagnostic Fracture Injection Test	Closure stress, reservoir pressure, near-wellbore transmissibility	Near-wellbore- to reservoir-scale	Closure identification non-unique; interpretation sensitive to fracture mechanics assumptions and non-ideal field conditions
Pressure Interference Testing	Interwell hydraulic connectivity, hydraulic diffusivity, fracture conductivity	Interwell-scale	High sensitivity to data noise; model non-uniqueness; scalability limited in complex multi-well configurations
Interwell Tracer Testing	Interwell connectivity, sweep efficiency, fracture network complexity	Interwell-scale	Semi-quantitative results; sensitive to tracer transport assumptions; requires pre-test simulation for reliable design
Single-well Tracer Testing	Near-wellbore fracture connectivity, stage contribution assessment	Near-wellbore-scale	Flow reversal and dispersion effects limit quantitative interpretation; unsuitable for highly heterogeneous reservoirs

2.1. Direct Fracture Diagnostic Technologies

Microseismic monitoring enables field-scale mapping of stimulated rock volume, yet it cannot independently verify fracture conductivity or fluid connectivity. DTS identifies fracture entry points and fluid distribution along the wellbore, although its interpretation remains highly model-dependent. DAS captures dynamic strain fields with high temporal resolution, but its performance is limited by uncertainties in fiber–formation coupling and directional sensitivity. Tiltmeter measurements provide reliable estimates of fracture orientation and volume; however, fracture size estimation becomes increasingly ill-posed in far-field deployments. Overall, these methods should be viewed as complementary rather than interchangeable, and their effective application depends on clearly defining the diagnostic objective.

2.1.1. Microseismic Monitoring

Microseismic monitoring (MSM) originates from earthquake seismology and has been adapted for subsurface engineering applications to directly detect small-scale seismic events induced by hydraulic fracturing. During stimulation, stress perturbations develop around propagating fracture tips, leading to tensile, shear, or mixed-mode failures that generate microseismic emissions. By recording event waveforms and accurately locating seismic sources, MSM provides direct observations of fracture activation and the spatial extent of stimulated rock volume.

Advances in seismic instrumentation enabled the transition of MSM from tectonic-scale monitoring to field-scale fracture diagnostics in unconventional reservoirs. Since the 1980s, MSM has been widely applied during hydraulic fracturing operations to evaluate treatment effectiveness, with metrics such as Effective Stimulation Volume (ESV) commonly used to estimate fracture extent [8]. As shown in Figure 1, the monitoring systems typically consist of surface, near-surface, or borehole sensor arrays designed to capture low-magnitude seismic signals generated during stimulation. Surface arrays offer the broadest spatial coverage and are the easiest to deploy, but signal attenuation through the overburden significantly reduces sensitivity, particularly for deep reservoirs, resulting in lower event detection rates and reduced location accuracy. Near-surface deployments, typically at shallow burial depths of tens to hundreds of meters, partially mitigate attenuation effects while retaining operational flexibility, offering an intermediate option where borehole access is limited. Downhole deployments, in which sensor arrays are placed in dedicated monitoring wells or temporarily deployed via wireline, provide the highest signal-to-noise ratio and event location accuracy due to proximity to the fracture zone, but are constrained by wellbore availability, cost, and limited spatial aperture. In practice, the choice of deployment configuration depends on reservoir depth, available infrastructure, and the required balance between areal coverage and detection sensitivity [9,10]. Consequently, optimized sensor configurations and integrated monitoring strategies are frequently employed to enhance event detection and localization accuracy.

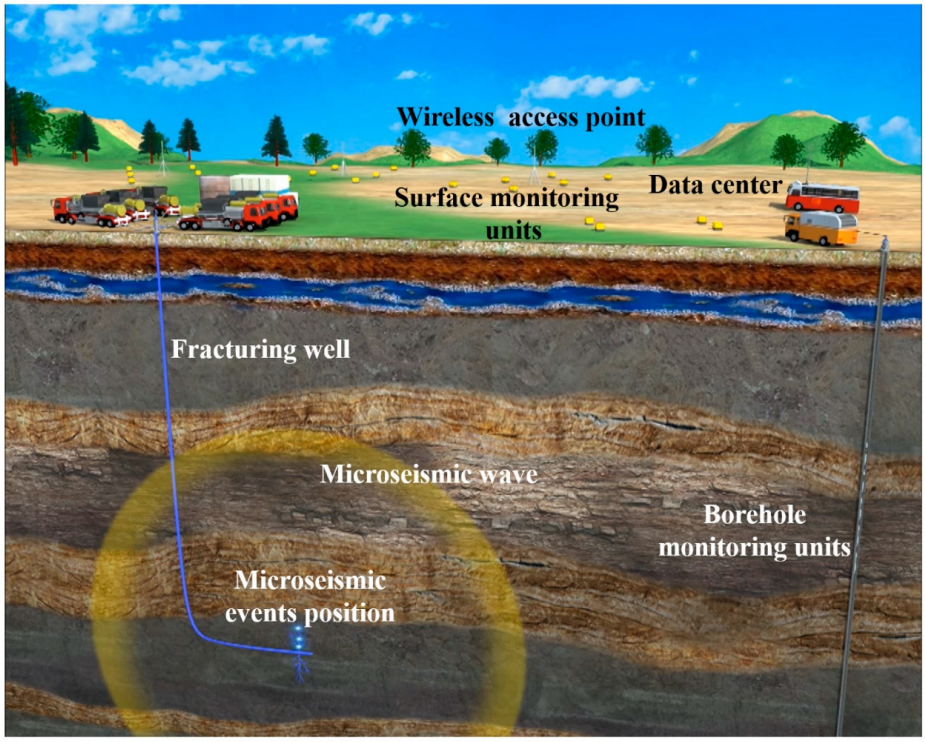


Figure 1. Schematic diagram of microseismic monitoring for hydraulic fracture diagnosis [11].

Extensive field studies have demonstrated the effectiveness of MSM in characterizing fracture geometry, fracture–fault interactions, and stimulation performance. Integration of MSM observations with static and time-lapsed three-dimensional Mechanical Earth Models (MEMs) has been shown to improve interpretation of fracture propagation and geomechanical response [12–15]. Case studies from shale plays such as the Barnett, Eagle Ford, Austin Chalk, and Sichuan Basin shales illustrate how spatial and temporal patterns of microseismicity can be used to assess fracture complexity, identify fault interactions, and optimize treatment design [16]. More recent work has further combined MSM data with fracture network modeling, well testing, and rock property analysis to constrain fracture geometry and validate stimulation effectiveness, even when seismic events occur away from the wellbore (Figure 2) [17,18].

Despite its maturity and widespread adoption, MSM has inherent limitations. Restricted sensor coverage can affect event location accuracy and source mechanism inversion, and microseismic observations alone cannot uniquely resolve fracture geometry without support from fracture mechanics and geomechanical modeling. In addition, distinguishing stimulation-induced seismicity from natural background events remains challenging [19]. While microseismic-derived SRV provides a spatial representation of the stimulated zone, it does not necessarily reflect the volume that effectively contributes to production. Defining ESV requires characterization of actual reservoir response, including stress state, mechanical properties, and flow behavior within the microseismicity field [20,21]. Attempts to bridge this gap have incorporated pressure-based diagnostics; for example, Quaglia et al. [21] estimated SRV in a shale formation using a finite element model constrained by DFIT pressure decline data. However, pressure-based approaches alone cannot confirm fluid connectivity or proppant placement within the stimulated zone. Tracer analysis and pressure interference testing offer complementary pathways to constrain ESV more reliably, by providing direct evidence of hydraulic connectivity and interwell communication that microseismic observations cannot independently resolve. These limitations underscore the importance of integrating MSM with complementary diagnostic data and advanced

modeling workflows. Recent developments, including machine learning-based signal classification and automated event detection, have shown promise in improving data quality and interpretation reliability [22].

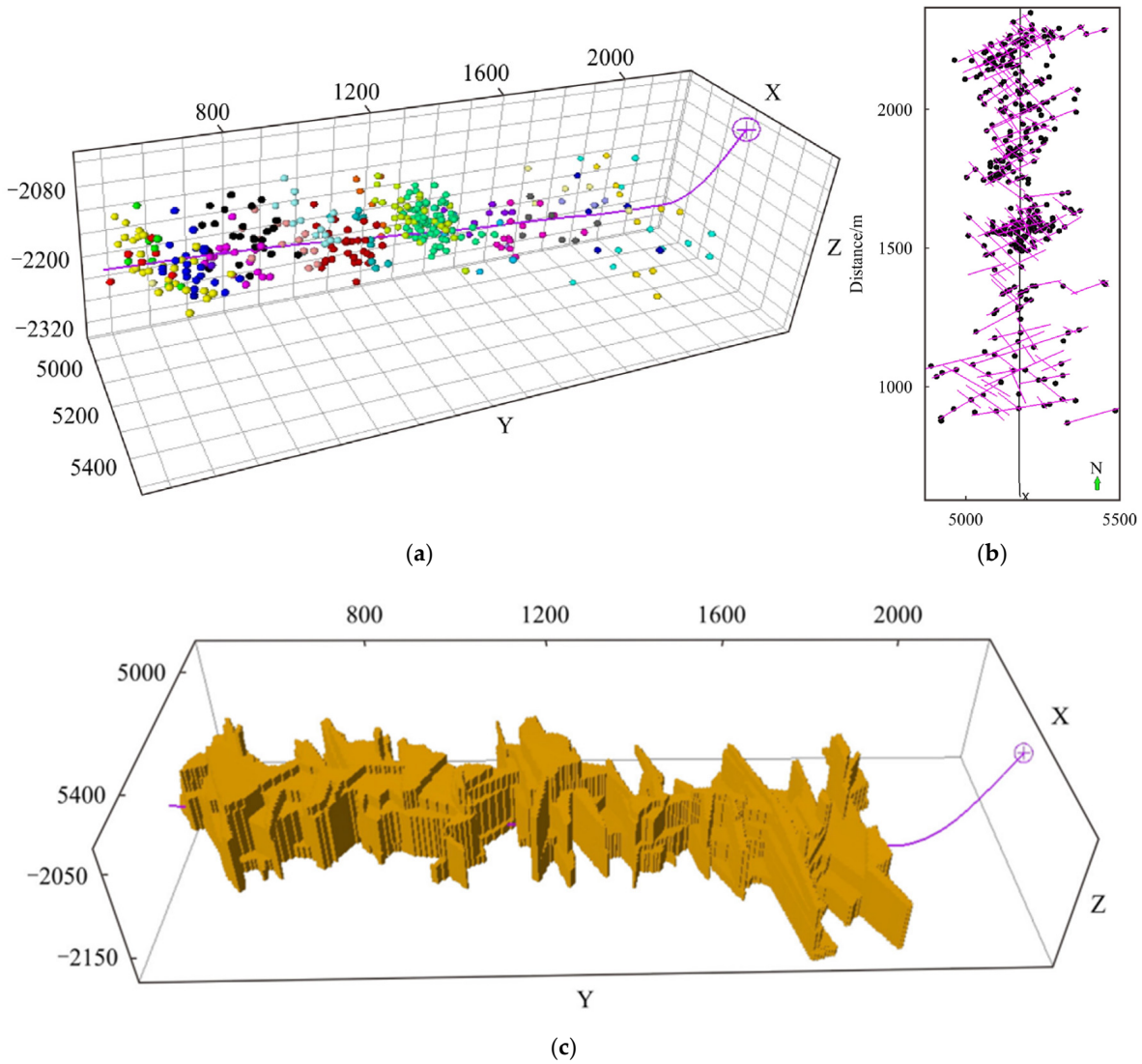


Figure 2. (**a**) Detected microseismic waveform (purple curves) shown along with sensor positions (green dots) across the downhole [9]; (**b**) 3D visualization of microseismic events and source locations around a horizontal well; (**c**) reconstruction of hydraulic fractures based on the recorded microseismic events [17].

2.1.2. Downhole Fiber Optics

Fiber-optic (FO) sensing was first introduced in the 1990s using single-point pressure and temperature measurements and has since evolved into a widely adopted downhole monitoring technology due to its cost-effectiveness and capability for continuous data acquisition [23]. In unconventional reservoirs characterized by high temperature and pressure, the long-term reliability of electronic sensors often degrades, limiting their applicability over the full production lifecycle [24]. In contrast, FO sensors have demonstrated robust performance under harsh downhole conditions, making them well suited for permanent wellbore monitoring [25]. A typical configuration of downhole FO monitoring system is shown in Figure 3.

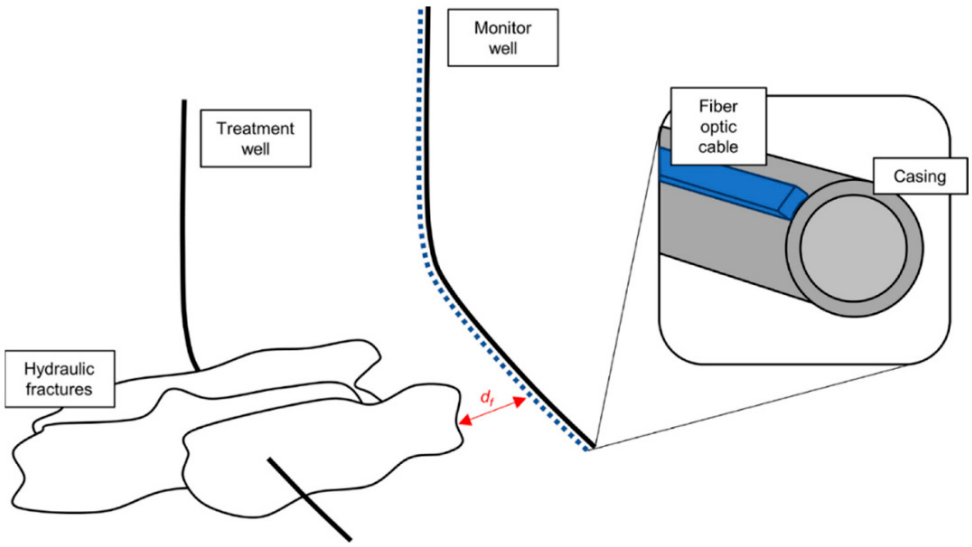


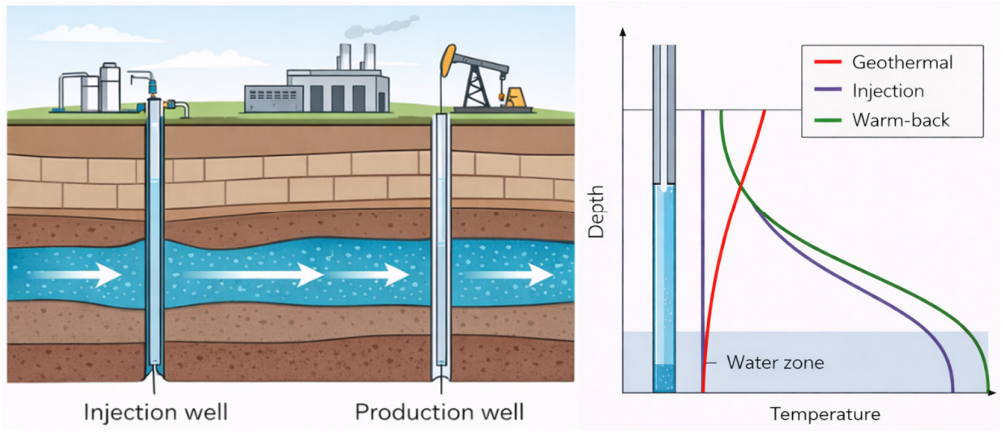
Figure 3. Schematic representation of downhole fiber optics in the far-field monitoring well [26].

FO sensing systems typically rely on cables deployed either temporarily via coiled tubing or wireline, or permanently cemented along the outside of the production casing. This configuration enables intervention-free and non-intrusive monitoring of wellbore activities throughout stimulation and production operations [23]. By utilizing distributed sensing principles, a single FO cable can function as a continuous array of sensing points, allowing spatially resolved measurements along the entire wellbore. Depending on the interrogation method and signal type, FO systems can be configured to capture temperature, acoustic, strain, or pressure-related responses [27].

These capabilities have led to the development of distributed fiber-optic sensing technologies, most notably distributed temperature sensing (DTS) and distributed acoustic sensing (DAS), which provide real-time, high-resolution measurements for downhole monitoring applications. As a result, FO sensing has become a practical foundation for establishing consistent production and stimulation diagnostics in unconventional reservoirs [28].

Distributed Temperature Sensing

The concept of Raman-scattering-based Distributed Temperature Sensing (DTS) was first introduced in 1984 and has been applied to downhole monitoring for more than two decades [29]. In fiber-optic sensing, backscattered light consists of Rayleigh, Brillouin, and Raman components, among which Raman scattering is most commonly used for DTS due to its high sensitivity to temperature variations. As an inelastic scattering process, Raman scattering arises from interactions between incident photons and molecular vibrations, producing Stokes and anti-Stokes signals whose intensity ratio is temperature dependent [30]. Although Raman-based DTS exhibits reduced sensitivity at lower temperatures and is less responsive to pressure and strain compared to Brillouin- and Rayleigh-based methods, it remains well suited for high-resolution temperature monitoring in hydraulic fracturing environments [31,32]. Figure 4 illustrates the characteristic temperature evolution during the geothermal, injection, and warm-back phases monitored using DTS.



(**a**) (**b**)

Figure 4. Schematic demonstration of temperature profile produced by DTS. (**a**) Subsurface geothermal system; (**b**) temperature profile vs. depth.

DTS provides direct measurements of distributed downhole temperature, enabling continuous and intervention-free monitoring throughout injection, shut-in, and production stages. Temperature perturbations caused by fracturing fluid injection, fluid entry into fractures, or fluid exchange with nonproductive zones can be clearly detected, allowing DTS to characterize fluid distribution and near-wellbore flow behavior [33]. Abnormal temperature profiles not only reflect fluid production but are also influenced by the Joule–Thomson effect, whereby gas expanding from high-pressure formation into the wellbore undergoes isenthalpic cooling, producing temperature anomalies that may be misinterpreted as fracture fluid entry points in gas-bearing intervals if not properly accounted for in DTS interpretation [34]. During injection and early shut-in, convective heat transfer dominates as the injected cold fluid flows along fracture pathways, suppressing temperature recovery in stimulated intervals. In the later shut-in period, thermal conduction becomes the primary mechanism, as residual cold fluid within fractures absorbs heat from the surrounding formation more slowly than unfractured intervals, producing the characteristic flattened temperature profiles observed in DTS measurements [35,36]. Representative examples of DTS-based temperature inversion and fracture geometry reconstruction are presented in Figures 5 and 6.

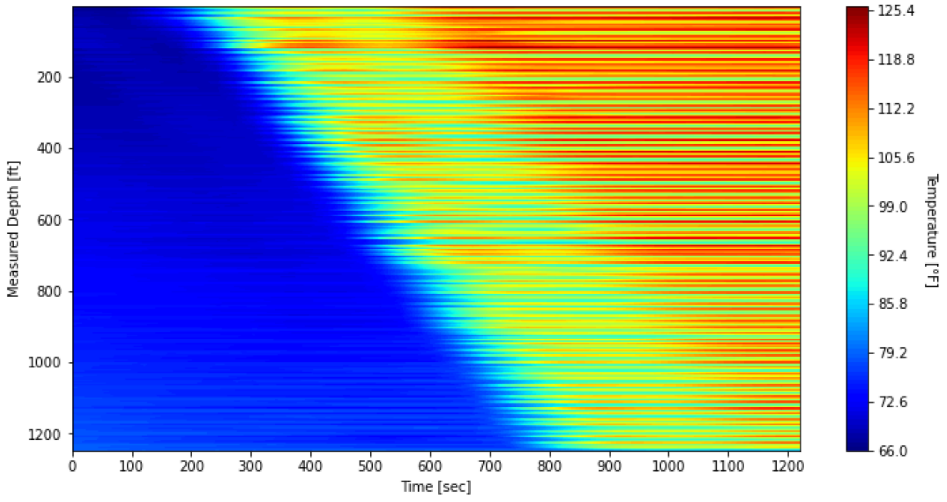
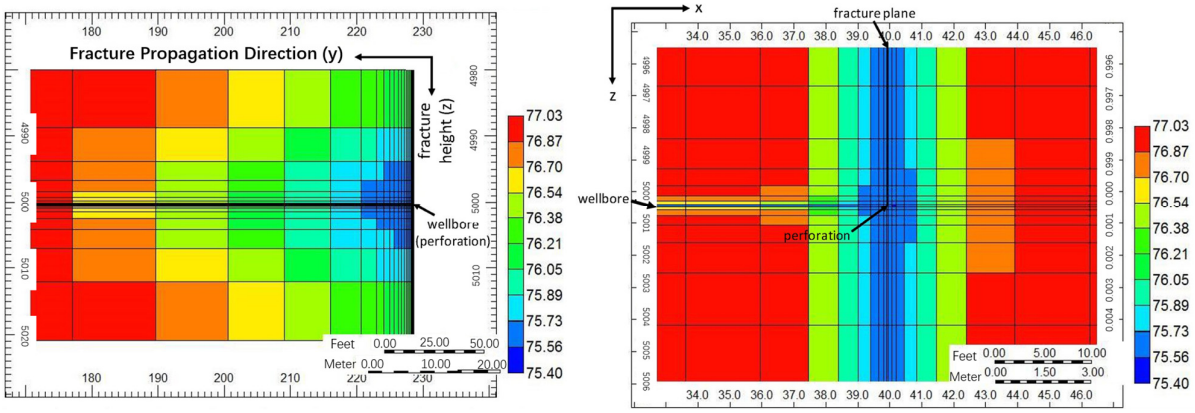


Figure 5. Temperature inversion from DTS signals to monitoring cooling during warm-up period [37].



(**a**) (**b**)

Figure 6. Schematic Illustration of temperature field around the perforation in fracture plane (**a**) and vertical view of wellbore (**b**), showing DTS-measured temperature profile during injection can be used to indicate fracture generation [38].

Based on this thermal response mechanism, a range of analytical, semi-analytical, and numerical inversion approaches have been developed to estimate fracture characteristics from DTS data. Early transient heat conduction models demonstrated the feasibility of inferring fracture extent and fluid penetration distance with acceptable accuracy [39]. Subsequent studies extended these approaches by incorporating wellbore–reservoir coupling, multiphase flow, heterogeneous reservoir properties, and complex fracture geometries. For example, Cui et al. [40] employed a semi-analytical thermal model to diagnose fractured-well performance, while Sun et al. [41] developed a fully coupled reservoir–wellbore framework validated against numerical simulators. More recently, Zhao et al. [42] integrated DTS observations with embedded discrete fracture models (EDFM) to quantify fracture length and width within complex fracture networks, demonstrating the potential of DTS for quantitative fracture diagnostics when supported by appropriate modeling frameworks.

Despite its demonstrated effectiveness, DTS-based fracture interpretation remains strongly model-dependent. Uncertainties in hydraulic fracture geometry, fluid–formation heat transfer, and multiphase flow behavior can propagate into inversion results, limiting the uniqueness and robustness of inferred fracture parameters. Moreover, fracture length and width derived from thermal data alone are often insufficient to fully characterize complex fracture networks. These limitations highlight the need for advanced fracture modeling, optimized inversion workflows, and integration with complementary diagnostic techniques to improve the reliability of DTS-based fracture diagnostics.

Distributed Acoustic Sensing

Distributed Acoustic Sensing (DAS) is a more recent fiber-optic-based monitoring technology compared to DTS and is built upon coherent optical time-domain reflectometry (C-OTDR). In DAS systems, short pulses of highly coherent light are transmitted along an optical fiber, and the Rayleigh backscattered signal is analyzed to detect dynamic strain-rate variations along the entire fiber length [43]. As an elastic scattering process, Rayleigh scattering is sensitive to vibration- and strain-induced perturbations without frequency shift, making DAS well suited for real-time acoustic and deformation monitoring with high spatial and temporal resolution [44]. As illustrated in Figure 7, DAS measurements recorded in the monitoring well reveal fracture-closure signals after injection ceases, while fracture hits generated during the previous stage remain detectable before pumping begins in the current stage.

Owing to its capability for continuous sampling in both space and time, DAS has significantly advanced well surveillance by enabling full-wellbore monitoring without discrete sensors [23]. In unconventional reservoirs, DAS has been applied to a wide range of hydraulic fracturing-related operations, including ball tracking, injection monitoring, perforation cluster efficiency evaluation, interstage and interwell communication detection, and production profiling [45]. In addition, DAS has been successfully used for time-lapse vertical seismic profiling (VSP) and for monitoring microseismic activity induced by hydraulic fracturing, further demonstrating its versatility as a direct sensing technology [46–51].

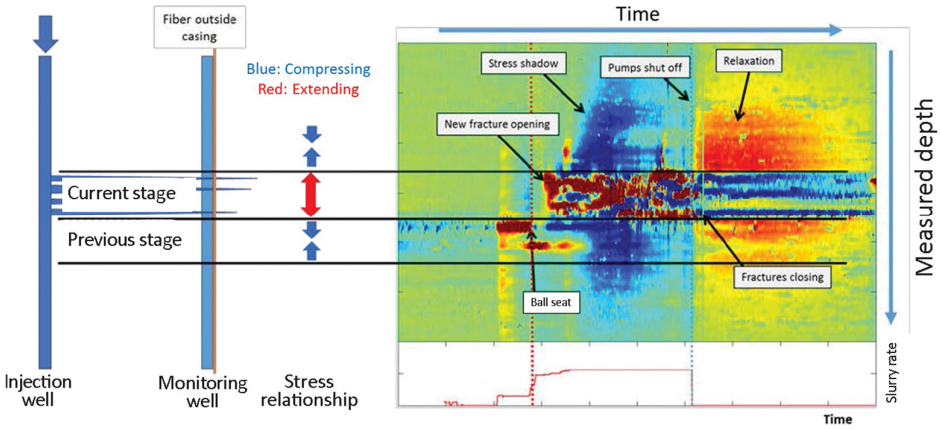


Figure 7. The illustration of LF-DAS response at an offset well during hydraulic fracturing [52].

For fracture diagnostics, DAS interpretation primarily focuses on low-frequency strain responses associated with fracture propagation rather than high-frequency wellbore noise. Raw DAS measurements often contain spurious signals generated by wellbore vibration, drilling activities, or interrogator noise. In contrast, fracture growth induces far-field strain perturbations characterized by extensional zones ahead of fracture tips and compressional zones adjacent to fracture planes [53]. Low-frequency DAS (LF-DAS) techniques have therefore been developed to isolate these strain-dominated responses and enhance fracture-related signal interpretation [54]. Figure 8 schematically illustrates the strain perturbations associated with fracture propagation. Early field studies demonstrated the feasibility of using cross-well LF-DAS to monitor hydraulic fracture geometry, establishing the foundation for subsequent model-based interpretation approaches [52].

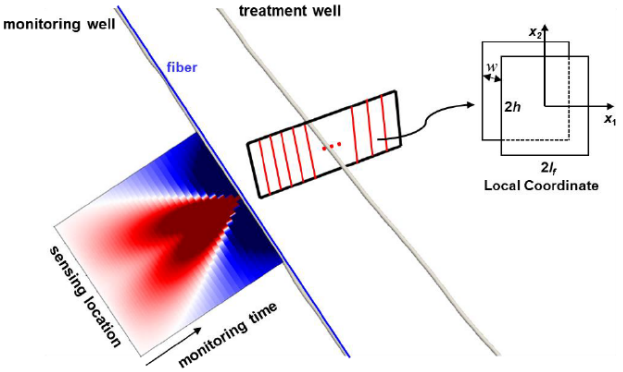


Figure 8. Schematic of discrete element method using LF-DAS-measured strain evolution to accommodate the varying fracture width and depth [55]. The blue-colored region represents low signal strength, whereas the red-colored region represents high signal strength.

Building on this concept, a range of numerical modeling and inversion methods have been proposed to quantitatively interpret LF-DAS observations. Compared with

Distributed Strain Sensing (DSS) based on Brillouin scattering, LF-DAS offers comparable sensitivity to strain-related phenomena while benefiting from simpler instrumentation and a unified DAS infrastructure. Existing studies can be broadly categorized into forward modeling of fracture-induced strain fields and inversion-based reconstruction of fracture geometry. Representative examples include Green's function-based inversion algorithms to estimate fracture length, width, height, and stimulated volume [45], sensitivity analyses examining the effects of fiber–fracture distance and well inclination [56], and gradient-based inversion frameworks capable of accommodating spatially varying fracture properties [55]. While these approaches have shown encouraging agreement with short-term field observations, discrepancies over longer monitoring periods highlight the need for improved model robustness and long-term validation.

Despite its growing adoption, DAS-based fracture diagnostics has not yet reached full maturity. Key challenges include limited directional sensitivity, complex amplitude responses, uncertainties associated with fiber–formation coupling, spatial positioning of fiber-optic cables, and the management of large data volumes generated during continuous monitoring [57]. Among these challenges, real-time data processing, signal classification, and feature extraction remain particularly critical. As a result, machine learning-based approaches for automated signal identification and intelligent interpretation are increasingly being explored as a promising direction for advancing DAS-based fracture diagnostics [58].

2.1.3. Tiltmeter Survey

Hydraulic fracturing perturbs the in situ stress field by increasing pore pressure, inducing measurable deformation in the surrounding formation. This deformation can be directly captured by tiltmeters deployed at the surface or in offset wells, providing a basis for fracture diagnostics through mechanical inversion of the observed strain field [59]. Fracture-induced stress changes propagate into the far field, and the resulting deformation magnitude is approximately proportional to fracture size, while fracture orientation is primarily controlled by the regional stress regime [60,61], as illustrated in Figures 9 and 10. With regional stress conditions constrained by tectonic stress–strain theory and geodetic observations [62], tiltmeter measurements enable estimation of fracture orientation, extent, and complexity during stimulation.

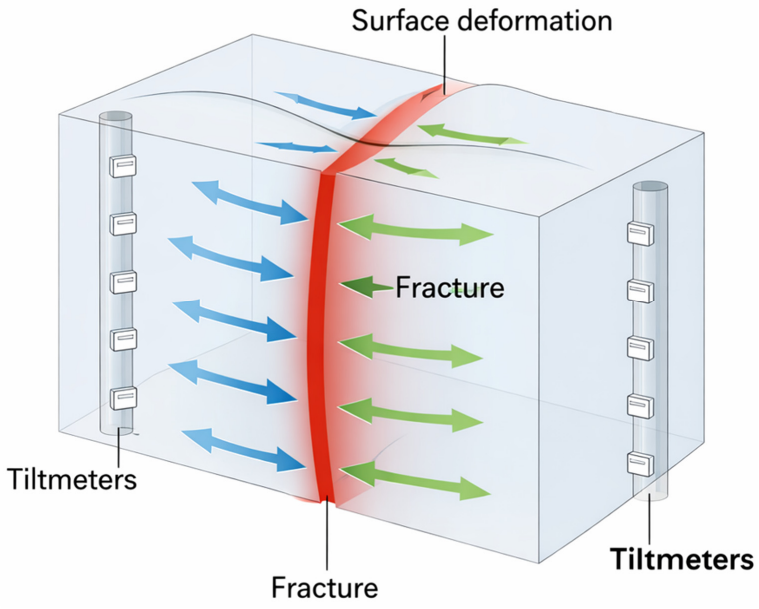


Figure 9. Principle of surface tiltmeter fracture mapping. The arrows represent rock deformation around the induced fracture.

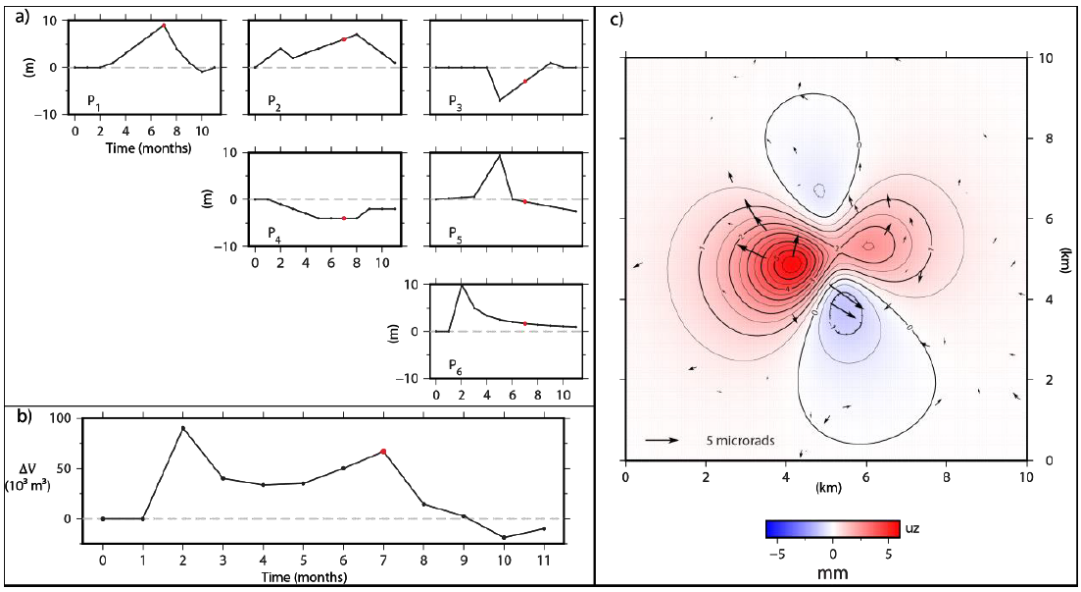


Figure 10. (**a**) Evolution of six components of strain tensor measured by surface tiltmeters; (**b**) evolution of fracture volume change over time; (**c**) vertical deformation (color scale) and synthetic tilts (black arrows) produced by the seismic event observed at surface at a given time step [63].

Tiltmeter-based fracture mapping was first explored in the late 1970s and became more widely applied by the late 1990s, particularly before the emergence of distributed fiber-optic sensing technologies. Arrays of surface or offset-well tiltmeters record the azimuth and magnitude of deformation at multiple locations, and the measured tilt responses are inverted to identify fracture parameters that best reproduce the observed data [64]. While surface tiltmeters are operationally simple and cost effective, their applicability is limited by depth-related signal attenuation and reduced resolution in deep reservoirs. To overcome these constraints, wireline-deployed downhole tiltmeters were introduced, significantly extending the usable depth range and improving signal-to-noise ratios through advances in instrument design and signal processing [65].

Despite these improvements, tiltmeter-based fracture diagnostics face fundamental challenges associated with nonlinear and over-constrained inversion. Lecampion et al. [66] demonstrated using displacement discontinuity modeling that when tiltmeters are located in the far field—typically beyond 1.5 times the fracture half-length—only fracture volume and orientation can be reliably inferred, while fracture size estimation becomes ill-posed without additional constraints. To address these limitations, advanced inversion strategies have been developed, including ensemble Kalman filter (EnKF) approaches to capture asymmetric fracture growth [67] and joint inversion of tiltmeter and microseismic data to reduce uncertainty in fracture geometry [68].

In unconventional reservoirs, the presence of complex fracture networks and interactions with natural fractures further complicates tiltmeter interpretation. To better resolve these effects, elastic forward modeling and Green's function-based inversion techniques have been applied to link observed deformation with fracture network evolution [69]. More recently, strain tensor-based inversion frameworks derived from Okada-type dislocation models have been proposed to characterize dominant deformation modes and volumetric changes within simplified representations of complex fracture networks [53]. These studies indicate that tiltmeter measurements effectively capture formation-scale deformation and fracture volume evolution, while reliable reconstruction of detailed fracture geometry generally requires additional constraints and integration with complementary diagnostic methods.

2.2. Indirect Fracture Detection Technologies

Diagnostic Fracture Injection Tests provide estimates of closure stress, reservoir pressure, and near-wellbore transmissibility, although interpretation remains sensitive to fracture mechanics assumptions and non-ideal field conditions. Pressure interference testing quantifies interwell hydraulic connectivity and fracture conductivity at the pad scale, with key challenges including high sensitivity to data noise and model non-uniqueness. Interwell tracer testing evaluates fracture network complexity and connectivity between wells, yet results remain semi-quantitative and require pre-test simulation for reliable design. Single-well tracer testing assesses near-wellbore fracture connectivity and stage contribution with minimal operational complexity, where flow reversal and dispersion effects represent the primary constraints on quantitative interpretability. Collectively, these methods provide diagnostic information that direct methods cannot capture, particularly regarding fracture conductivity and interwell connectivity, and are most effective when deployed alongside direct diagnostic observations.

2.2.1. Diagnostic Fracture Injection Test (DFIT)

Early attempts to infer fracture properties from pressure transient behavior were pioneered by Nolte [70–72], who demonstrated that post-injection pressure decline could be used to estimate fracture closure and fluid-loss behavior under simplified assumptions of fracture geometry and leak-off. The introduction of the G-function enabled practical interpretation of pressure data by normalizing shut-in time with respect to cumulative leak-off potential, forming the foundation for pressure-based fracture diagnostics [73,74].

These concepts led to the widespread use of fluid-loss or "mini-frac" tests in conventional reservoirs, where small, controlled fractures were induced to support fracture treatment design through estimation of in situ stress and leak-off characteristics. However, the applicability of traditional mini-frac analysis is limited in unconventional reservoirs, where heterogeneous lithology, anisotropic stress conditions, and complex fracture networks violate key assumptions such as stable fracture propagation and symmetric fracture growth.

To address these limitations, mini-frac concepts were adapted into Diagnostic Fracture Injection Tests (DFITs), which shift the emphasis from fracture geometry prediction to fracture diagnostics based on pressure decay behavior following shut-in. Although DFITs evolved from mini-frac testing, the two are not equivalent, as DFITs typically involve limited injection volumes and short durations that preclude stable fracture growth. This design choice simplifies the fracture system, allowing the pressure response to more cleanly reflect intrinsic reservoir parameters—such as closure stress, pore pressure, and near-wellbore transmissibility—without interference from complex fracture geometry. Figure 11 illustrates the typical DFIT workflow, which can be conceptually divided into five sequential stages: (1) injection begins with surface pumps compressing the wellbore fluid until formation breakdown pressure is reached, initiating a hydraulic fracture; (2) fluid continues to be injected at a constant rate to propagate the fracture until pressure stabilization indicates the end of fracture extension; (3) the injection is abruptly stopped, and the instantaneous shut-in pressure (ISIP) is recorded, marking the transition to the pressure falloff phase; (4) during the early shut-in period, pressure decline is monitored to evaluate fracture closure behavior, typically associated with changes in fracture compliance and used to identify the minimum horizontal stress; and (5) late-time falloff data are analyzed using after-closure analysis (ACA) to identify flow regimes and estimate key reservoir properties.

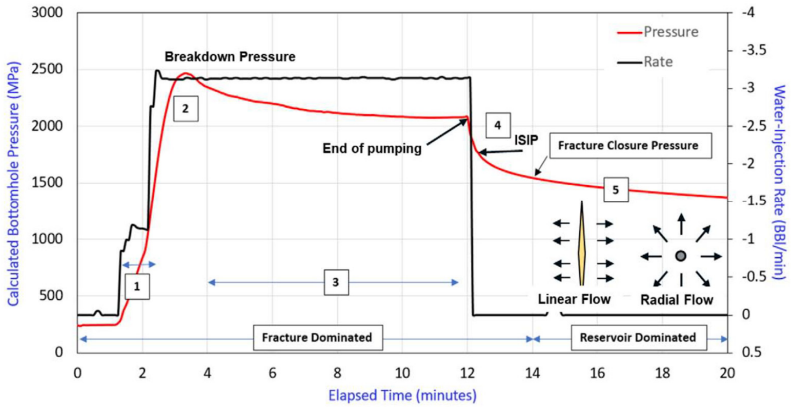


Figure 11. Schematic demonstration of five pressure falloff stages during DFIT data analysis [75].

Consequently, DFIT interpretation focuses on estimating reservoir pore pressure, fracture closure stress, fracture compliance, and near-wellbore transmissibility rather than direct fracture geometry. Over time, DFITs have become a standard pressure-based diagnostic tool in unconventional reservoir development. Nevertheless, the interpretation of DFIT data remains strongly model-dependent, and the reliability of inferred parameters is influenced by assumptions regarding fracture mechanics, leak-off behavior, and reservoir heterogeneity. These challenges motivate continued refinement of DFIT analysis methods and underscore the need for careful application and integration with complementary diagnostic techniques, as discussed in the following sections.

Extension of DFIT Toward Flow Back Analysis (DFIT-FBA)

Standard DFIT operating procedures have been well documented in the literature, encompassing test objective definition, injection design, execution, and pressure falloff interpretation [76–79]. A typical DFIT involves controlled injection to initiate a small hydraulic fracture, abrupt shut-in to record instantaneous shut-in pressure (ISIP), early-time pressure falloff analysis to evaluate fracture closure behavior, and late-time ACA) to estimate reservoir pressure and near-wellbore transmissibility. The differences between the DFIT and DFIT-FBA workflows are illustrated in Figure 12.

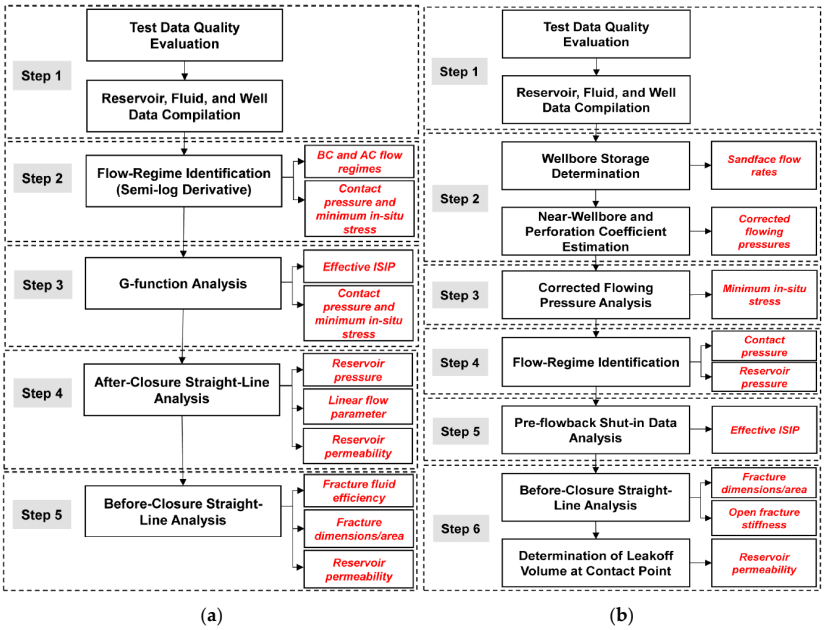


Figure 12. Summary of workflow for shut-in data analysis with conventional DFIT (**a**) and DFIT-FBA (**b**) [80].

To extend the diagnostic value of DFITs beyond shut-in analysis, flowback analysis (FBA) has been increasingly integrated into DFIT workflows. FBA examines pressure and rate responses during controlled early flowback to assess fracture closure behavior, near-wellbore conductivity, and fracture–reservoir connectivity. While flowback-based diagnostics—often referred to as "dynamic closure tests" or extended leak-off tests (XLOTs)—have been applied in the industry for decades, their importance has become more pronounced in unconventional reservoirs, where well performance depends critically on fracture conductivity rather than matrix flow alone [81].

Recent DFIT-FBA designs emphasize single-cycle injection and controlled flowback to minimize fluid–rock interaction effects and avoid mechanical alteration caused by repeated pressurization. Studies have shown that fluid–shale interactions can significantly impact fracture permeability, leading to biased interpretation of closure pressure and transmissibility if multiple injection cycles are used [82]. Consequently, DFIT-FBA procedures are increasingly designed as "one-go" tests, combining injection, shut-in, and flowback within a single operation.

By applying rate-transient analysis (RTA) to flowback pressure and rate data, DFIT-FBA enables identification of flow regimes associated with fracture closure and fluid-bank evolution, allowing estimation of fracture conductivity, reservoir pressure, and near-wellbore productivity. Field applications have demonstrated that DFIT-FBA can significantly reduce testing time—from days to hours—while providing early diagnostic insights critical for unconventional and frontier developments [83,84].

Despite these advantages, DFIT-FBA interpretation remains subject to ongoing debate. The identification of fracture closure from flowback-derived flow regimes is sensitive to residual fluid effects and model assumptions, leading to uncertainty in inferred closure pressure and fracture properties [85]. In addition, optimal design of injection and flowback parameters remains case-specific and difficult to generalize due to limited a priori knowledge of reservoir properties. Recent efforts have addressed these challenges through uncertainty-aware analytical modeling and sensitivity analysis, highlighting the need for tailored DFIT-FBA design rather than reliance on fixed operational guidelines [86].

More recent developments have extended DFIT-FBA concepts to multi-well settings and integrated workflows, enabling estimation of fracture parameters, reservoir permeability, and SRV at the pad or field scale [87]. While numerical and analytical models continue to advance, the reliability of DFIT-FBA interpretations ultimately depends on field validation, underscoring the need for further studies using high-quality flowback test data.

Common Data Acquisition and Interpretation Issues in DFIT and Flowback Tests

Past field applications have demonstrated that DFIT and flowback-based diagnostics are highly sensitive to both data acquisition practices and interpretation assumptions, often leading to non-unique or misleading results if not carefully designed and analyzed.

Data acquisition–related issues are among the most common sources of uncertainty. Previous studies have reported that the use of non-Newtonian or wall-building fluids, insufficient falloff duration, unaccounted wellbore temperature effects, and inappropriate injection-rate protocols can significantly distort pressure responses and mask reservoir flow regimes [88,89]. In flowback-based diagnostics, inaccurate measurement of sandface flowback rates and near-wellbore friction further complicate the interpretation of fracture closure and transmissibility [80,90].

Interpretation-related challenges primarily stem from oversimplified assumptions regarding fracture geometry and pressure behavior. Multiple studies have shown that traditional methods for identifying ISIP and fracture closure pressure—such as tangent line or semi-log G-function approaches—can become invalid in tight formations where

near-wellbore pressure losses, natural fracture activation, and fracture interference are significant [75,91,92]. The presence of multiple inflection points and ambiguous derivative signatures often leads to overinterpretation of pseudo-radial or linear flow regimes.

Non-ideal field effects further complicate DFIT analysis in unconventional reservoirs. Time-dependent rock deformation (creep), poroelastic stress interactions between adjacent wells, fracture-to-fracture communication, and falling liquid-level effects can introduce transient behaviors that deviate from classical DFIT assumptions [93]. These phenomena highlight the limitations of purely pressure-based diagnostics when applied without additional constraints.

Collectively, these issues underscore that reliable DFIT and DFIT-FBA interpretation requires careful test design, high-quality data acquisition, and physically defensible interpretation workflows. Best practices increasingly emphasize hypothesis testing through full-physics simulations and integration with complementary diagnostics to reduce non-uniqueness and mitigate the risk of misinterpretation.

2.2.2. Pressure Interference Testing

From Classical Type-Curve Matching to Pressure Interference Testing

Pressure interference testing has long been used to characterize reservoir connectivity and transmissibility through analysis of pressure responses observed in offset wells. Its conceptual foundation originates from groundwater hydrology studies in the early twentieth century, where analytical solutions such as the Theis recovery curve were developed to describe pressure diffusion caused by well pumping [94]. These early solutions, based on line-source theory, later formed the basis for pressure transient analysis techniques adopted in the petroleum industry.

To account for additional complexities encountered in oil and gas reservoirs—including wellbore storage, skin effects, and transient flow behavior—type-curve matching methods were introduced, most notably by Jacob [95]. By fitting field pressure data to analytical solutions under prescribed boundary and initial conditions, type-curve analysis enabled estimation of key reservoir parameters such as permeability–thickness, storativity, and skin. Subsequent developments, including pressure-derivative analysis, improved the identification of flow regimes and enhanced diagnostic capability [96].

Despite their widespread use, classical type-curve methods rely on simplifying assumptions that limit their applicability in fractured and heterogeneous reservoirs. The presence of faults, natural fractures, and induced fracture networks introduces additional flow paths and transient behaviors that cannot be adequately captured by conventional line-source solutions. To address some of these challenges, Abbaszadeh et al. [97] extended interference-test interpretation to faulted reservoirs by decoupling matrix and fault flow contributions. While effective for idealized single-fault scenarios, such approaches remain sensitive to model assumptions and interpreter judgment, particularly in the presence of data noise and complex fracture systems [98].

These inherent limitations of classical type-curve matching and pressure interference analysis have motivated the development of more advanced interpretation methodologies that incorporate fracture geometry, reservoir heterogeneity, and data-driven workflows. Recent advances in pressure interference testing aim to reduce non-uniqueness, improve robustness, and extend diagnostic capability to unconventional reservoirs, as discussed in the following sections.

Applications and Recent Advancement of Pressure Interference Testing

Recent advancements in pressure interference testing have focused on improving the characterization of interwell connectivity in unconventional reservoirs, where com-

plex fracture networks and non-Fickian flow behavior limit the applicability of classical pressure transient models. Figure 13 illustrates a typical pressure interference testing workflow, while Figure 14 presents example fracture-hit configurations obtained through data inversion.

One major development is the introduction of power-law diffusion-based metrics to quantify fracture connectivity. Chu et al. [99,100] proposed the Chow Pressure Group (CPG), which characterizes the temporal scaling of pressure interference and captures the magnitude and evolution of pressure communication between wells. Unlike conventional flow models, CPG provides a robust, qualitative measure of connectivity degradation over time and has been shown to correlate with well spacing and fracture interference in multi-fractured horizontal wells. Building on this concept, Almasoodi et al. [101] introduced the Devon Quantification of Interference (DQI) metric through numerical simulation, demonstrating its ability to estimate hydraulic diffusivity and fracture conductivity. Subsequent work by Ponners et al. [102] clarified the relationship between CPG and DQI, investigated plateau behavior at long times, and extended the framework to multi-well pad configurations, thereby improving scalability beyond two-well systems.

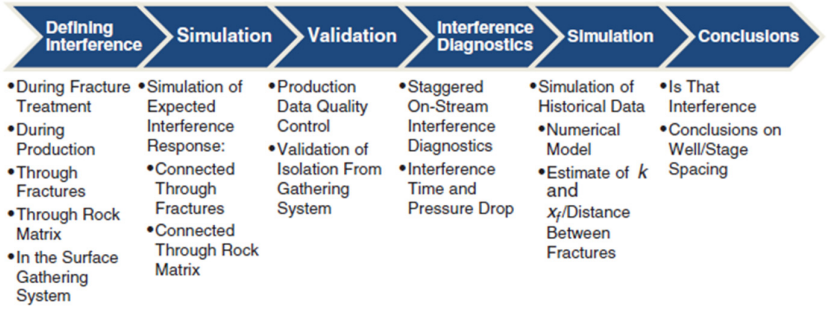


Figure 13. Testing workflow of the interference test [103].

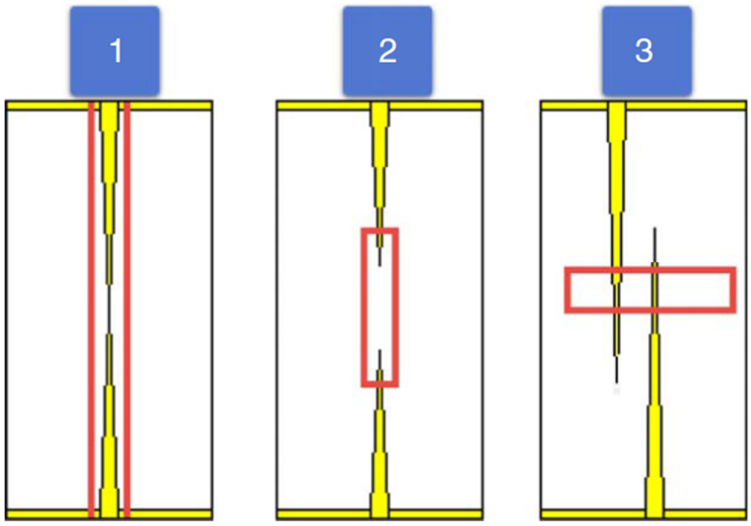


Figure 14. Different fracture-hit configurations that can cause interference [103].

In parallel, advanced reservoir models have been incorporated into pressure interference interpretation. Gavrilov et al. [104] demonstrated that dual-porosity formulations can capture flow behavior that single-porosity models fail to represent, enabling separate evaluation of matrix and fracture properties. Such approaches highlight the importance of explicitly accounting for fracture–matrix interaction when interpreting interference responses in fractured shale reservoirs.

Another important area of advancement is data conditioning and normalization. Pressure interference analysis is highly sensitive to production fluctuations and operational disturbances, which can obscure true reservoir responses. To address this challenge, Liu et al. [105] developed a pressure deconvolution algorithm that normalizes dynamic production data prior to interpretation. Their results showed improved type-curve convergence and more reliable estimation of fracture parameters and interwell connectivity, although further refinement is needed to account for multiphase flow effects.

Despite these advances, pressure interference testing continues to face challenges related to data noise, model non-uniqueness, and computational scalability. Future developments are expected to focus on integrating high-resolution monitoring data, improving physics-based and uncertainty-aware modeling frameworks, and combining interference metrics with Bayesian inference and physics-informed machine learning. Collectively, these advancements aim to enhance the robustness and practical applicability of pressure interference diagnostics for optimized well spacing, completion design, and long-term reservoir development planning in unconventional plays.

2.2.3. Tracer Analysis

Background and Practical Considerations

Tracer techniques have been applied in oilfield operations since the 1940s as diagnostic tools for drilling, completion, and reservoir characterization. Early studies demonstrated the use of radioactive tracers to investigate fluid movement, fracture presence, and permeability variations in subsurface formations, establishing tracer analysis as a practical alternative to direct measurements in complex reservoirs. With continued development, tracer methods evolved into more systematic diagnostic approaches through the introduction of interwell tracer tests (IWTT) and single-well tracer tests (SWTT) [106,107], which enabled estimation of residual phase saturation and assessment of reservoir connectivity beyond the capabilities of conventional core analysis and logging.

IWTT relies on tracer transport between injector–producer pairs under a consistent flow direction, allowing quantitative evaluation of interwell connectivity and sweep efficiency at the reservoir scale [108,109]. In contrast, SWTT is conducted within a single well and provides near-wellbore diagnostic information with minimal operational complexity [110]. Although SWTT interpretation is more sensitive to reservoir heterogeneity, dispersion, and flow reversal effects, its rapid deployment and relatively low cost make it attractive for early-stage evaluation and surveillance in unconventional reservoirs. Together, IWTT and SWTT form the foundation of tracer-based diagnostics for fracture characterization and connectivity assessment.

The effectiveness of tracer analysis depends on the use of tracers that are chemically and physically stable under reservoir conditions, exhibit predictable transport or partitioning behavior, and minimize interaction with reservoir fluids and rock [111–114]. In practice, tracer selection is highly formation specific and is constrained by reservoir temperature, fluid composition, environmental considerations, and detection requirements. Among the various tracer types, radioactive tracers have been widely applied in hydraulic fracturing diagnostics due to their high thermal stability, sensitivity at low concentrations, and compatibility with standard logging tools, enabling reliable identification of fracture fluid distribution and treatment effectiveness when managed within acceptable safety limits [115].

Given the diversity of available tracer materials and the frequent lack of disclosure in field applications, this review does not attempt a comprehensive comparison of tracer chemistries. Instead, the following sections focus on tracer-based diagnostic methodologies—specifically IWTT and SWTT—and their application to fracture characterization, interwell connectivity evaluation, and performance assessment in unconventional

reservoirs, where tracer responses provide indirect but valuable insights into subsurface fracture networks.

Interwell Tracer Testing (IWTT)

Early reviews of interwell tracer testing (IWTT) highlighted that test failure is often attributable to inadequate sampling, empirical decision-making, and the absence of pre-test simulation, underscoring the importance of systematic workflow design [116]. These challenges are amplified in unconventional shale reservoirs, where fracture-driven flow dominates and tracer transport behavior deviates significantly from assumptions developed for conventional systems.

Subsequent studies have increasingly focused on improving IWTT design and interpretation through integration with fracture diagnostics and numerical modeling. King and Leonard [117] demonstrated the use of proppant tracers during zipper fracturing to reveal significant interwell fracture interference, illustrating the potential of tracer data to diagnose fracture connectivity at the wellbore scale. However, incomplete disclosure of tracer selection and test preparation in early field studies highlighted the need for standardized design and reporting practices.

To address design uncertainty, physics-based modeling approaches have been introduced to support tracer test planning. Tian et al. [118] developed a modified random walk particle tracking (RWPT) algorithm for multiphase tracer transport, showing improved performance over one-dimensional models, although simplifications limited direct field applicability. More recent studies have integrated tracer transport into embedded discrete fracture models (EDFM), enabling characterization of complex fracture networks and sensitivity analysis of fracture orientation, length, and connectivity [119]. These models demonstrated consistency with field-scale tracer tests and highlighted the strong dependence of tracer recovery on fracture geometry.

At the field scale, tracer data have increasingly been used as complementary constraints in multi-well hydraulic fracturing models. Albrecht et al. [120] showed that incorporating tracer recovery into history-matching workflows improved estimation of fracture propagation and well spacing optimization in large multi-well systems. To reduce operational complexity associated with multiple tracers, Jain et al. [121] proposed stage-based tracer injection strategies that enable assessment of interwell connectivity while minimizing tracer demand. Additional applications have employed residence time distribution analysis and reversibly adsorbing tracers to qualitatively assess fracture network heterogeneity and estimate fracture surface area, with observed correlations to production performance [122,123].

Collectively, these studies indicate that IWTT is most effective for qualitative to semi-quantitative evaluation of interwell connectivity and fracture network complexity. While advanced modeling and optimized test design have significantly improved interpretability, IWTT results remain sensitive to tracer transport assumptions, fracture heterogeneity, and operational uncertainties. Consequently, IWTT is best applied in conjunction with pressure-based diagnostics and fracture monitoring techniques to provide a more comprehensive assessment of stimulated reservoir behavior.

Single-Well Tracer Testing (SWTT)

Compared to IWTT, SWTT is generally less suitable for highly heterogeneous reservoirs, as tracer recovery during flowback is not guaranteed and interpretation is strongly influenced by flow-field reversal and dispersion effects [124,125]. These challenges complicate the relationship between tracer residence time, reservoir volume, and fracture geometry, limiting the quantitative capability of traditional SWTT approaches.

To improve SWTT interpretability, several studies have introduced physics-based modeling frameworks that explicitly account for fracture flow and tracer transport. Ghergut et al. [126] developed a conservative tracer-based method to quantify discharge from individual fractures during multi-stage flowback, enabling assessment of inflow uniformity in unconventional reservoirs. Subsequent studies extended this concept by incorporating more realistic fracture representations. Kumar and Sharma [127] integrated the Barton–Bandis fracture closure model within a multi-fracture simulation framework, demonstrating that tracer returns from individual stages correlate with their contribution to cumulative production. This approach was further expanded using embedded discrete fracture models (EDFM) to investigate the impact of fracture network geometry, conductivity, and adsorption behavior on tracer concentration responses [128,129]. While these model-based methods show promise for quantitative fracture diagnostics, their accuracy remains sensitive to assumptions regarding tracer–fluid–rock interactions and fracture connectivity.

In parallel, SWTT has been increasingly applied as a qualitative diagnostic tool for field-scale hydraulic fracturing evaluation. Tian et al. [130] proposed a residence time distribution-based analysis to infer fracture network complexity and stimulated reservoir volume from tracer mixing behavior in produced fluids. More recently, chemical tracers have been used as intervention-less alternatives to production logging tools, enabling stage-by-stage assessment of production contribution, well cleanup, and operational anomalies during early flowback [131]. These approaches prioritize rapid decision-making over detailed geometric inversion and are particularly valuable in operational settings where conventional logging is impractical.

Advances in tracer technology have further expanded the applicability of SWTT. To address limitations of conventional chemical tracers—such as thermal degradation, phase partitioning, and adsorption—novel materials including nano-encapsulated DNA tracers and solid-phase dye-colored proppants have been developed, offering improved stability and detectability under harsh reservoir conditions [132,133]. These innovations enhance the robustness of tracer-based diagnostics and broaden their application scope beyond traditional flowback analysis.

Overall, SWTT is best suited for qualitative to semi-quantitative assessment of near-wellbore fracture connectivity, stage contribution, and fracture network complexity. While recent advances in modeling and tracer materials have improved diagnostic capability, SWTT remains complementary to interwell tracer testing and pressure-based diagnostics, particularly in heterogeneous unconventional reservoirs where non-uniqueness and operational uncertainty persist.

2.3. AI-Driven Fracture Diagnostics: From Automated Interpretation to Predictive Intelligence

While the integration of fracture diagnostic techniques has been extensively reviewed in previous studies, recent advances have increasingly focused on the application of artificial intelligence (AI) and machine learning (ML) to enable automated, predictive, and real-time fracture characterization. Traditional fracture diagnostics often rely on interpreter-dependent workflows and simplified assumptions, limiting scalability and consistency across heterogeneous datasets. In this context, AI-driven methods have emerged as a promising pathway to enhance diagnostic integration, reduce human bias, and support data-intensive decision-making [7]. Figure 15 summarizes the general workflow of ML applications in fracture diagnostics. Given that AI applications in fracture diagnostics have been extensively reviewed elsewhere, this section provides a brief overview of emerging directions rather than a comprehensive technical assessment.

Early applications of AI in fracture diagnostics primarily targeted automated interpretation of pressure-based data, particularly DFIT and pressure transient analysis (PTA).

Machine learning models have demonstrated the ability to infer fracture properties directly from pressure–time responses without explicit specification of fracture geometry or detailed geomechanical inputs. Recent examples include neural network-based estimation of fracture geometry and conductivity from treatment parameters and production behavior [134], as well as signal-processing-assisted DFIT interpretation frameworks that improve robustness to noise and enable near-real-time analysis [135]. Building on the wavelet-based pressure-transient analysis introduced by Soliman et al. [136], Gabry et al. [137] developed a continuous wavelet transform (CWT)-based method for pressure and water hammer signal analysis that overcomes the limitations of G-function interpretation and enables more accurate and robust fracture closure detection. These approaches highlight the potential of AI to streamline routine diagnostic tasks and accelerate operational workflows.

Beyond single-well diagnostics, AI has been increasingly applied to spatially complex fracture characterization problems. Pattern recognition and data-driven inversion techniques have been used to reconstruct fracture networks and connectivity from microseismic and deformation data, providing intuitive representations of fracture–fracture and fracture–wellbore interactions [138]. Inversion-based studies have further combined Bayesian inference, surrogate modeling, and evolutionary optimization to address long-standing challenges of non-uniqueness and data scarcity in fracture geometry estimation from tiltmeter and pressure measurements [139,140]. These developments suggest that AI-enhanced inversion can transform traditionally qualitative diagnostics into probabilistic, uncertainty-aware quantitative tools.

AI-assisted methods have also been extended to interwell connectivity detection and field-scale performance prediction. Recurrent neural networks and data-fusion frameworks have been used to identify intra-pad and inter-pad fracture hits, particularly in parent–child well scenarios, enabling early intervention and optimized well spacing decisions [138]. At larger scales, supervised ML algorithms have been trained on physics-informed datasets to predict hydraulic fracturing performance, although challenges related to generalization, uncertainty quantification, and real-time applicability remain [141,142].

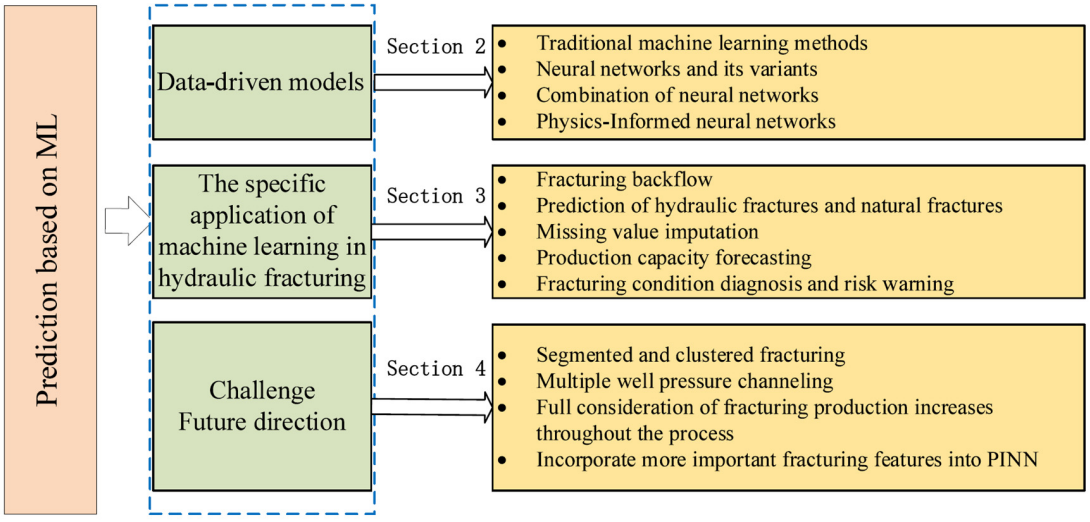


Figure 15. ML application workflow in fracture diagnosis [142].

To address these limitations, recent research has increasingly emphasized physics-informed and hybrid AI frameworks. Physics-informed neural networks (PINNs) embed governing physical laws directly into the learning process, improving interpretability and reducing reliance on large, labeled datasets. When combined with transfer learning and physics-based forward simulations, PINNs offer a promising pathway to bridge the gap

between data-driven flexibility and physical realism in fracture diagnostics [143,144]. Recent studies have demonstrated that integrating machine learning (ML) with finite element analysis (FEM) represents a promising direction for addressing the computational bottlenecks and modeling challenges associated with hydraulic fracture propagation and inverse parameter identification [145–148]. Wan et al. [149] compared conventional FEM and physics-informed neural network (PINN) approaches, showing that the predicted fracture growth patterns, propagation velocities, and magnitudes were highly consistent between the two methods, while the PINN framework significantly reduced computational cost. Compared with conventional FEM-based explicit algorithms, the proposed PINN approach improved computational efficiency by simplifying constitutive relation calculations during fracture simulation. However, because the study was conducted under relatively simplified modeling scenarios, the applicability and predictive accuracy of the framework for complex field-scale hydraulic fracturing processes still require further validation.

To improve the adaptability of PINN-based frameworks under more realistic fracturing conditions, Ryu et al. [150] developed a moving boundary PINN (MB-PINN) model that incorporated extensive validation datasets across different fracture propagation scenarios. By introducing moving boundary constraints, the MB-PINN framework provided greater flexibility in representing the influence of varying formation and fluid properties on fracture behavior. In addition, the dual-neural-network formulation reduced parametric dependencies compared with conventional PINN approaches, thereby extending the applicability of the model to more heterogeneous reservoir conditions.

Building upon these developments, Chen et al. [151] proposed a DeepONet-embedded physics-informed neural network (DE-PINN) to further address the limitations of conventional PINN architectures in learning complex multiscale transport behaviors. While MB-PINN primarily improves the representation of evolving fracture boundaries and coupled physical processes, DE-PINN further enhances operator-level learning and generalization capability for multiscale and heterogeneous hydraulic fracturing systems. In this architecture, the forward network predicts production behavior using geological and fracture parameters, whereas the sampling network incorporates the spatial coordinates of training sample points constrained by partial differential equations (PDEs). By combining operator learning with physics-based constraints, the DE-PINN framework improves the characterization of hydraulic fracture morphology and multiscale transport mechanisms within both the shale matrix and fracture network. Moreover, the enhanced generalization capability of the DE-PINN model enables broader application across varying reservoir conditions without requiring repeated retraining. Collectively, these advances indicate a paradigm shift toward AI-augmented fracture diagnostics, where direct observations and indirect measurements are integrated through joint inversion, feature fusion, and physics-informed learning to support predictive and real-time decision-making in unconventional reservoir development.

However, despite the substantial improvements in computational efficiency demonstrated by PINN-FEM integration methods, several technical challenges still hinder their full-scale adoption in both research and industry. Many models rely heavily on idealized or simulation-derived datasets with limited representation of geological heterogeneity and coupled multi-physics processes, restricting their applicability to complex field conditions. Generalization across different fracture geometries, boundary conditions, and reservoir scenarios also remains limited, while the black-box nature of many deep learning models reduces interpretability and physics-based transparency. In addition, uncertainty quantification and validation protocols are often insufficiently addressed, particularly under realistic field-scale conditions. Practical deployment is further constrained by limited inter-

operability with conventional FEM platforms and the high computational cost associated with training high-fidelity PINN and surrogate models [152].

3. Conclusions

This review has presented a comprehensive assessment of hydraulic fracture diagnostic technologies used in unconventional reservoirs, with the objective of clarifying their physical foundations, practical applicability, and inherent limitations. By systematically examining both direct diagnostics—such as microseismic monitoring, fiber-optic sensing, and tiltmeter measurements—and indirect methods based on pressure, production, and tracer data, this work provides a unified perspective that addresses long-standing fragmentation in diagnostic understanding and practice.

The analysis demonstrates that the reliability of individual diagnostic techniques is often constrained by modeling assumptions, data quality, and non-ideal field conditions. Direct measurements offer valuable insights into fracture behavior but remain subject to non-uniqueness and interpretation uncertainty, particularly in complex fracture networks. Indirect diagnostics continue to play a critical role in evaluating fracture closure and interwell connectivity, yet their effectiveness depends on robust acquisition protocols and physically consistent interpretation frameworks.

A central contribution of this review is the proposal of a mechanism-oriented classification framework that distinguishes diagnostic methods by their underlying physical sensing principles rather than by instrument type alone. This distinction reveals a systematic pattern: direct methods are generally more sensitive to fracture geometry and deformation-related responses, whereas indirect methods are often more informative regarding fracture conductivity and hydraulic connectivity. Furthermore, the explicit classification of indirect diagnostics into single-well and multi-well application modes offers a structured basis for deployment decisions that is absent from existing reviews. Notably, the inclusion of pressure interference testing as a formal diagnostic category alongside established methods reflects its growing relevance in multi-well unconventional development, where interwell communication critically affects completion design and production performance. The integration of multiple diagnostics and the application of physics-informed AI remain important directions for future development and have been extensively discussed in prior literature. The framework proposed here is intended to support more consistent and informed diagnostic selection across the multidisciplinary teams involved in unconventional reservoir development.

Author Contributions: Conceptualization, T.B. and G.Q.; methodology, T.B.; validation, G.Q. and M.Y.S.; formal analysis, T.B.; investigation, T.B.; writing—original draft preparation, T.B.; writing—review and editing, G.Q. and M.Y.S.; visualization, T.B.; supervision, G.Q.; project administration, G.Q. and M.Y.S. All authors have read and agreed to the published version of the manuscript.

Funding: This research received no external funding.

Data Availability Statement: The data presented in this study is available on request from the corresponding author.

Conflicts of Interest: The authors declare no conflicts of interest.

Abbreviations

The following abbreviations are used in this manuscript:

MSM	Microseismic Monitoring
SRV	Stimulated Reservoir Volume
ESV	Effective Stimulation Volume

FO	Fiber Optic
DTS	Distributed Temperature Sensing
VSP	Vertical Seismic Profiling
DAS	Distributed Acoustic Sensing
DSS	Distributed Strain Sensing
DFIT	Diagnostic Fracture Injection Test
ACA	After-Closure Analysis
PTA	Pressure Transient Analysis
FBA	Flowback Analysis
ISIP	Instantaneous Shut-In Pressure
IWTT	Interwell Tracer Testing
SWTT	Single-Well Tracer Testing
CPG	Chow Pressure Group
DQI	Devon Quantification of Interference
AI	Artificial Intelligence
ML	Machine Learning
PINN	Physics-Informed Neural Network
FEM	Finite Element Analysis
MB	Moving Boundary
DE	DeepONet-Embedded
PDEs	Partial Derivation Equations

References

1. Adekola, U.; Gimba, A.; Salihu, A.; Jakada, K.; Okafor, I.; Nzerem, P.; Chior, J.; Ogolo, O.; Ibrahim, K. A Comprehensive Review of Hydraulic Fracturing Techniques in Shale Gas Production. *Nile J. Eng. Appl. Sci.* **2023**, *1*, 216–228. [CrossRef]
2. Eshkalak, M.O.; Aybar, U.; Sepehrnoori, K. An Economic Evaluation on the Re-Fracturing Treatment of the U.S. Shale Gas Resources. In *Proceedings of the SPE Eastern Regional Meeting, Charleston, WV, USA, October 2014*; SPE: Richardson, TX, USA, 2014. [CrossRef]
3. Reynolds, D.B.; Umekwe, M.P. Shale-oil development prospects: The role of shale-gas in developing shale-oil. *Energies* **2019**, *12*, 3331. [CrossRef]
4. Tao, J.; Meng, S.; Cao, G.; Gao, Y.; Liu, H. Experimental study on the impact of supercritical CO_2 soak pre-treatment on re-fracturing of shale oil reservoirs. In *SPE Asia Pacific Oil and Gas Conference and Exhibition*; SPE: Richardson, TX, USA, November 2020; p. D023S012R001.
5. Hyman, J.D.; Jiménez-Martínez, J.; Viswanathan, H.S.; Carey, J.W.; Porter, M.L.; Rougier, E.; Karra, S.; Kang, Q.; Frash, L.; Chen, L.; et al. Understanding hydraulic fracturing: A multi-scale problem. *Philos. Trans. R. Soc. A Math. Phys. Eng. Sci.* **2016**, *374*, 20150426. [CrossRef]
6. Webster, P.; Cox, B.; Molenaar, M. Developments in diagnostic tools for hydraulic fracture geometry analysis. In *Global Meeting Abstracts*; Society of Exploration Geophysicists: Tulsa, OK, USA, 2013; pp. 218–224.
7. Mahmoud, A.; Gowida, A.; Aljawad, M.S.; Al-Ramadan, M.; Ibrahim, A.F. Advancement of hydraulic fracture diagnostics in unconventional formations. *Geofluids* **2021**, *2021*, 4223858. [CrossRef]
8. Inamdar, A.A.; Malpani, R.; Atwood, K.; Brook, K.; Erwemi, A.M.; Ogundare, T.M.; Purcell, D. Evaluation of stimulation techniques using microseismic mapping in the Eagle Ford Shale. In *Proceedings of the SPE Unconventional Resources Conference/Gas Technology Symposium*; SPE: Richardson, TX, USA, November 2010; p. SPE-136873.
9. Peyret, O.; Drew, J.; Mack, M.; Brook, K.; Maxwell, S.C.; Cipolla, C.L. Subsurface To Surface Microseismic Monitoring for Hydraulic Fracturing. In *Proceedings of the SPE Annual Technical Conference and Exhibition*; SPE: Richardson, TX, USA, 2012. [CrossRef]
10. Cipolla, C.L.; Fitzpatrick, T.; Williams, M.J.; Ganguly, U. Seismic-to-Simulation for Unconventional Reservoir Development. In *Proceedings of the SPE Reservoir Characterisation and Simulation Conference and Exhibition*; SPE: Richardson, TX, USA, 2011. [CrossRef]
11. Zhang, X.; Lin, J.; Chen, Z.; Sun, F.; Zhu, X.; Fang, G. An efficient neural-network-based microseismic monitoring platform for hydraulic fracture on an edge computing architecture. *Sensors* **2018**, *18*, 1828. [CrossRef]
12. Alexander, T.; Baihly, J.; Boyer, C.; Clark, B.; Waters, G.; Jochen, V.; Le Calvez, J.; Lewis, R.; Miller, C.K.; Thaeler, J.; et al. Shale gas revolution. *Oilfield Rev.* **2011**, *23*, 40–55.
13. Yu, C.; Shapiro, S. Seismic anisotropy of shale: Inversion of microseismic data. In *SEG International Exposition and Annual Meeting*; SEG: Tulsa, OK, USA, 2014; p. SEG-2014.

14. Leaney, W.S. Microseismic Source Inversion in Anisotropic Media. Ph.D. Thesis, University of British Columbia, Vancouver, BC, Canada, 2014.
15. Williams, M.J.; Le Calvez, J.H.; Conners, S.; Xu, W. Integrated microseismic and geomechanical study in the Barnett Shale Formation. *Geophysics* **2016**, *81*, KS135–KS147. [CrossRef]
16. Le Calvez, J.; Malpani, R.; Xu, J.; Stokes, J.; Williams, M. Hydraulic fracturing insights from microseismic monitoring. *Oilfield Rev.* **2016**, *28*, 16–33.
17. Ou, C.; Liang, C.; Li, Z.; Luo, L.; Yang, X. 3D visualization of hydraulic fractures using micro-seismic monitoring: Methodology and application. *Petroleum* **2022**, *8*, 92–101. [CrossRef]
18. Martyushev, D.A.; Yang, Y.; Kazemzadeh, Y.; Wang, D.; Li, Y. Understanding the mechanism of hydraulic fracturing in naturally fractured carbonate reservoirs: Microseismic monitoring and well testing. *Arab. J. Sci. Eng.* **2024**, *49*, 8573–8586. [CrossRef]
19. Li, L.; Tan, J.; Wood, D.A.; Zhao, Z.; Becker, D.; Lyu, Q.; Shu, B.; Chen, H. A review of the current status of induced seismicity monitoring for hydraulic fracturing in unconventional tight oil and gas reservoirs. *Fuel* **2019**, *242*, 195–210. [CrossRef]
20. Warpinski, N.R.; Wolhart, S. A Validation Assessment of Microseismic Monitoring. In *Proceedings of the SPE Hydraulic Fracturing Technology Conference, The Woodlands, TX, USA, 9–11 February 2016*; SPE: Richardson, TX, USA, 2016. [CrossRef]
21. Quaglia, A.I.; Medina, A.; Obstfeld, S.; D'hers, S. Stimulated Reservoir Volume (SRV) Estimation in the Vaca Muerta Formation Using a Geomechanical Permeability Evolution Law and Microseismic Monitoring Correlation. In *Proceedings of the SPE Hydraulic Fracturing Technology Conference and Exhibition*; SPE: Richardson, TX, USA, 2026. [CrossRef]
22. Anikiev, D.; Birnie, C.; bin Waheed, U.; Alkhalifah, T.; Gu, C.; Verschuur, D.J.; Eisner, L. Machine learning in microseismic monitoring. *Earth-Sci. Rev.* **2023**, *239*, 104371. [CrossRef]
23. Molenaar, M.M.; Cox, B.E. Field cases of hydraulic fracture stimulation diagnostics using fiber optic distributed acoustic sensing (DAS) measurements and Analyses. In *Proceedings of the SPE Middle East Unconventional Resources Conference and Exhibition*; SPE: Richardson, TX, USA, January 2013; p. SPE-164030.
24. Tiku, S.; Veneruso, A.F.; Etchells, R.K.; Pecht, M. Risk factors in oil and gas well electronics compared to other electronic industries. *Oil Gas. Sci. Technol.* **2005**, *60*, 721–730. [CrossRef]
25. Lu, P.; Lalam, N.; Badar, M.; Liu, B.; Chorpening, B.T.; Buric, M.P.; Ohodnicki, P.R. Distributed optical fiber sensing: Review and perspective. *Appl. Phys. Rev.* **2019**, *6*, 041302. [CrossRef]
26. Reid, T.; Li, G.; Zhu, D.; Hill, A.D. Experimental Investigation of Low-Frequency Distributed Acoustic Sensor Responses to Two Parallel Propagating Fractures. *Sensors* **2024**, *24*, 3880. [CrossRef]
27. Yao, Y.; Yan, M.; Bao, Y. Measurement of cable forces for automated monitoring of engineering structures using fiber optic sensors: A review. *Autom. Constr.* **2021**, *126*, 103687. [CrossRef]
28. Ugueto, G.A.; Todea, F.; Daredia, T.; Wojtaszek, M.; Huckabee, P.T.; Reynolds, A.; Laing, C.; Chavarria, J.A. Can you feel the strain? DAS strain fronts for fracture geometry in the BC Montney, Groundbirch. In *Proceedings of the SPE Annual Technical Conference and Exhibition*; SPE: Richardson, TX, USA, 2019; p. D021S029R005.
29. Dakin, J.P.; King, A.J. Limitations of a single-optical-fibre fluorimeter system due to background fluorescence. In *IEE Proceedings H (Microwaves, Optics and Antennas*; IEEE: Piscataway, NJ, USA, 1984; Volume 131, pp. 273–275.
30. Gardner, B.; Matousek, P.; Stone, N. Temperature Spatially Offset Raman Spectroscopy (T-SORS): Subsurface Chemically Specific Measurement of Temperature in Turbid Media Using Anti-Stokes Spatially Offset Raman Spectroscopy. *Anal. Chem.* **2015**, *88*, 832–837. [CrossRef]
31. Liu, D.; Ngo, N.Q.; Tjin, S.C.; Dong, X. A dual-wavelength fiber laser sensor system for measurement of temperature and strain. *IEEE Photonics Technol. Lett.* **2007**, *19*, 1148–1150. [CrossRef]
32. Schenato, L. A review of distributed fibre optic sensors for geo-hydrological applications. *Appl. Sci.* **2017**, *7*, 896. [CrossRef]
33. Yoshida, N.; Hill, A.D.; Zhu, D. Comprehensive modeling of downhole temperature in a horizontal well with multiple fractures. *Spe J.* **2018**, *23*, 1580–1602. [CrossRef]
34. de Waele, A.T.A.M. Basics of Joule–Thomson Liquefaction and JT Cooling. *J. Low Temp. Phys.* **2017**, *186*, 385–403. [CrossRef]
35. Ashry, I.; Mao, Y.; Wang, B.; Frode Hveding Bukhamseen Ahmed, Y.; Tien Khee Ng Ooi, B.S. A Review of Distributed Fiber–Optic Sensing in the Oil and Gas Industry. *J. Light. Technol.* **2021**, *40*, 1407–1431. [CrossRef]
36. Tabatabaei, M.; Zhu, D. Fracture-stimulation diagnostics in horizontal wells through use of distributed-temperature-sensing technology. *SPE Prod. Oper.* **2012**, *27*, 356–362. [CrossRef]
37. Nakamoto, R.; Leggett, S. Development of a Transient Wellbore Heat Transfer Model Validated with Distributed Temperature Sensing Data. *Sensors* **2025**, *25*, 6583. [CrossRef]
38. Mao, Y.; Zeidouni, M.; Godefroy, C.; Gysen, M. Fracture diagnostic using distributed temperature measurements during a pause in flow-back period. *J. Pet. Sci. Eng.* **2020**, *185*, 106632. [CrossRef]
39. Tabatabaei, M.; Tan, X.; Hill, A.D.; Zhu, D. Well performance diagnosis with temperature profile measurements. In *Proceedings of the SPE Annual Technical Conference and Exhibition*; SPE: Richardson, TX, USA, 2011; p. SPE-147448.

40. Cui, J.; Zhu, D.; Jin, M. Diagnosis of production performance after multistage fracture stimulation in horizontal wells by downhole temperature measurements. *SPE Prod. Oper.* **2016**, *31*, 280–288. [CrossRef]
41. Sun, H.; Yu, W.; Sepehrnoori, K. A new comprehensive numerical model for fracture diagnosis with distributed temperature sensing DTS. In *Proceedings of the SPE Annual Technical Conference and Exhibition?* SPE: Richardson, TX, USA, 2017; p. D011S002R002.
42. Zhao, Z.; Yang, H.; Wu, J.; Chang, C.; Sun, H.; Sepehrnoori, K.; Yu, W.; Torres, F.; Xavier, M. Fracture Diagnosis with Distributed Temperature Sensing Using Thermal Embedded Discrete Fracture Model (EDFM). In *ARMA US Rock Mechanics/Geomechanics Symposium*; ARMA: Houston, TX, USA, 2021; p. ARMA-2021.
43. Hill, D. Distributed acoustic sensing (DAS): Theory and applications. In *Frontiers in Optics*; Optica Publishing Group: Washington, DC, USA, 2015; p. FTh4E-1.
44. Boyd, R.W. The Nature of the Nonlinear Optical Susceptibility. In *Laser Sources and Applications*; CRC Press: Boca Raton, FL, USA, 2020; pp. 1–13.
45. Liu, Y. Hydraulic Fracture Geometry Characterization Using Low-Frequency Distributed Acoustic Sensing Data: Forward Modeling, Inverse Modeling, and Field Applications. Ph.D. Thesis, Texas A&M University, College Station, TX, USA, 2021.
46. Byerley, G.; Monk, D.; Aaron, P.; Yates, M. Time-lapse seismic monitoring of individual hydraulic frac stages using a downhole DAS array. *Lead. Edge* **2018**, *37*, 802–810. [CrossRef]
47. Binder, G.; Chakraborty, D. Detecting microseismic events in downhole distributed acoustic sensing data using convolutional neural networks. In *SEG Technical Program Expanded Abstracts 2019*; Society of Exploration Geophysicists: Tulsa, OK, USA, 2019; pp. 4864–4868.
48. Titov, A.; Binder, G.; Jin, G.; Tura, A.; Aaron, P.; Yates, M.; Gunnell, A. Analysis of scattered waves observed in inter-stage DAS VSP data from zipper-fracturing operations. In *SEG Technical Program Expanded Abstracts 2020*; Society of Exploration Geophysicists: Tulsa, OK, USA, 2020; pp. 3793–3797.
49. Karrenbach, M.; Kahn, D.; Cole, S.; Ridge, A.; Boone, K.; Rich, J.; Silver, K.; Langton, D. Hydraulic-fracturing-induced strain and microseismic using in situ distributed fiber-optic sensing. *Lead. Edge* **2017**, *36*, 837–844. [CrossRef]
50. Cole, S.; Karrenbach, M.; Kahn, D.; Rich, J.; Silver, K.; Langton, D. Source parameter estimation from DAS microseismic data. In *SEG International Exposition and Annual Meeting*; Society of Exploration Geophysicists: Tulsa, OK, USA, 2018; p. SEG-2018.
51. Vera Rodriguez, I.; Wuestefeld, A. Strain microseismics: Radiation patterns, synthetics, and moment tensor resolvability with distributed acoustic sensing in isotropic media. *Geophysics* **2020**, *85*, KS101–KS114. [CrossRef]
52. Jin, G.; Roy, B. Hydraulic-fracture geometry characterization using low-frequency DAS signal. *Lead. Edge* **2017**, *36*, 975–980. [CrossRef]
53. Grechka, V. Penny-shaped fractures revisited. *Stud. Geophys. Et Geod.* **2005**, *49*, 365–381. [CrossRef]
54. Peruzzo, C.; Simoni, L.; Schrefler, B.A. On stepwise advancement of fractures and pressure oscillations in saturated porous media. *Eng. Fract. Mech.* **2019**, *215*, 246–250. [CrossRef]
55. Liu, Y.; Liang, L.; Zeroug, S. Enhancing Understanding of Hydraulic Fracture Tip Advancement through Inversion of Low-Frequency Distributed Acoustic Sensing Data. *arXiv* **2023**, arXiv:2305.13138. [CrossRef]
56. Srinivasan, A.; Liu, Y.; Wu, K.; Jin, G.; Moridis, G. Geomechanical modeling of fracture-induced vertical strain measured by distributed fiber-optic strain sensing. *SPE Prod. Oper.* **2023**, *38*, 537–551.
57. Zhu, H.H.; Liu, W.; Wang, T.; Su, J.W.; Shi, B. Distributed acoustic sensing for monitoring linear infrastructures: Current status and trends. *Sensors* **2022**, *22*, 7550. [CrossRef] [PubMed]
58. Ma, Y.; Eaton, D.; Igonin, N.; Wang, C. Machine learning-assisted processing workflow for multi-fiber DAS microseismic data. *Front. Earth Sci.* **2023**, *11*, 1096212. [CrossRef]
59. Jeffrey, R.G.; Van As, A.; Zhang, X.; Bunger, A.P.; Chen, Z.R. Measurement of hydraulic fracture growth in a naturally fractured orebody for application to preconditioning. In *Caving 2010: Proceedings of the Second International Symposium on Block and Sublevel Caving*; Australian Centre for Geomechanics: Perth, WA, Australia, 2010; pp. 647–662.
60. Shuck, L.Z. Method for Selectively Orienting Induced Fractures in Subterranean Earth Formations. U.S. Patent 4005750, 1 February 1977.
61. Montgomery, C.T.; Smith, M.B. Hydraulic fracturing: History of an enduring technology. *J. Pet. Technol.* **2010**, *62*, 26–40. [CrossRef]
62. Angelier, J. Determination of the mean principal directions of stresses for a given fault population. *Tectonophysics* **1979**, *56*, T17–T26. [CrossRef]
63. Furst, S.; Chery, J.; Peyret, M.; Mohammadi, B. Tiltmeter data inversion to characterize a strain tensor source at depth: Application to reservoir monitoring. *J. Geod.* **2020**, *94*, 48. [CrossRef]
64. Wright, C.A.; Davis, E.J.; Minner, W.A.; Ward, J.F.; Weijers, L.; Schell, E.J.; Hunter, S.P. Surface tiltmeter fracture mapping reaches new depths-10,000 feet and beyond. In *Proceedings of the SPE Rocky Mountain Petroleum Technology Conference/Low-Permeability Reservoirs Symposium*; SPE: Richardson, TX, USA, 1998; p. SPE-39919.

65. Castillo, D.; Hunter, S.; Harben, P.; Wright, C.; Conant, R.; Davis, E. Deep hydraulic fracture imaging: Recent advances in tiltmeter technologies. *Int. J. Rock. Mech. Min. Sci.* **1997**, *34*, 47.e1–47.e9. [CrossRef]
66. Lecampion, B.; Jeffrey, R.; Detournay, E. Resolving the geometry of hydraulic fractures from tilt measurements. *Pure Appl. Geophys.* **2005**, *162*, 2433–2452. [CrossRef]
67. Pandurangan, V.; Chen, Z.; Jeffrey, R.G. Mapping hydraulic fractures from tiltmeter data using the ensemble Kalman filter. *Int. J. Numer. Anal. Methods Geomech.* **2016**, *40*, 546–567. [CrossRef]
68. Du, J.; Brissenden, S.J.; McGillivray, P.R.; Bourne, S.; Hofstra, P.; Davis, E.J.; Roadarmel, W.H.; Wolhart, S.L.; Marsic, S.; Gusek, R.W.; et al. Mapping reservoir volume changes during cyclic steam stimulation using tiltmeter-based surface-deformation measurements. *SPE Reserv. Eval. Eng.* **2008**, *11*, 63–72. [CrossRef]
69. Astakhov, D.K.; Roadarmel, W.H.; Nanayakkara, A.S. A new method of characterizing the stimulated reservoir volume using tiltmeter-based surface microdeformation measurements. In *SPE Hydraulic Fracturing Technology Conference and Exhibition*; SPE: Richardson, TX, USA, 2012; p. SPE-151017.
70. Nolte, K.G. Determination of fracture parameters from fracturing pressure decline. In *Proceedings of the SPE Annual Technical Conference and Exhibition*; SPE: Richardson, TX, USA, 1979; p. SPE-8341.
71. Nolte, K.G. A general analysis of fracturing pressure decline with application to three models. *SPE Form. Eval.* **1986**, *1*, 571–583. [CrossRef]
72. Nolte, K.G. Principles for fracture design based on pressure analysis. *SPE Prod. Eng.* **1988**, *3*, 22–30. [CrossRef]
73. Castillo, J.L. Modified fracture pressure decline analysis including pressure-dependent leakoff. In *Proceedings of the SPE Rocky Mountain Petroleum Technology Conference/Low-Permeability Reservoirs Symposium*; SPE: Richardson, TX, USA, 1987; p. SPE-16417.
74. Gulrajani, S.N.; Nolte, K.G.; Economides, M.J. Chapter 9: Fracture evaluation using pressure diagnostics. In *Reservoir Stimulation*; John Wiley: Chichester, UK; New York, NY, USA, 2000.
75. Mohamed, M.I.; Salah, M.; Coskuner, Y.; Ibrahim, M.; Pieprzica, C.; Ozkan, E. Investigation of non-ideal diagnostic fracture injection tests behavior in unconventional reservoirs. In *Proceedings of the SPE Hydraulic Fracturing Technology Conference and Exhibition*; SPE: Richardson, TX, USA, 2019; p. D021S005R006.
76. Marongiu-Porcu, M.; Ehlig-Economides, C.A.; Economides, M.J. Global model for fracture falloff analysis. In *Proceedings of the SPE Unconventional Resources Conference/Gas Technology Symposium*; SPE: Richardson, TX, USA, 2011; p. SPE-144028.
77. Soliman, M.Y.; Gamadi, T. Testing tight gas and unconventional formations and determination of closure pressure. In *Proceedings of the SPE/EAGE European Unconventional Resources Conference and Exhibition*; SPE: Richardson, TX, USA, 2012; p. SPE-150948.
78. Cramer, D.D.; Nguyen, D.H. Diagnostic fracture injection testing tactics in unconventional reservoirs. In *Proceedings of the SPE Hydraulic Fracturing Technology Conference and Exhibition*; SPE: Richardson, TX, USA, 2013; p. D011S003R003.
79. Wallace, J.; Kabir, C.S.; Cipolla, C.L. Multiphysics investigation of diagnostic fracture injection tests in unconventional reservoirs. In Proceedings of the SPE Hydraulic Fracturing Technology Conference, The Woodlands, TX, USA, 4–6 February 2014; p. SPE-168620.
80. Clarkson, C.R.; Zeinabady, D.; Zanganeh, B.; Haqparast, S. Learnings from Over 5 Years of Design, Implementation, and Analysis of the Modified Flowback DFIT, DFIT-FBA. In *Proceedings of the SPE Hydraulic Fracturing Technology Conference and Exhibition*; SPE: Richardson, TX, USA, 2025; p. D021S004R002.
81. Varela, R.A.; Maniere, J.L. Successful dynamic closure test using controlled flow back in the Vaca Muerta formation. In *Proceedings of the SPE Argentina Exploration and Production of Unconventional Resources Symposium*; SPE: Richardson, TX, USA, 2016; p. D011S003R003.
82. Bai, T.; Hashemi, S.; Melkoumian, N.; Badalyan, A.; Zeinijahromi, A. Permeability Evolution of Shale during High-Ionic-Strength Water Sequential Imbibition. *Energies* **2024**, *17*, 3598. [CrossRef]
83. Zanganeh, B.; Clarkson, C.R.; Hawkes, R.R.; Jones, J.R. A new DFIT procedure and analysis method: An integrated field and simulation study. *J. Nat. Gas Sci. Eng.* **2019**, *63*, 10–17. [CrossRef]
84. Zanganeh, B.; Clarkson, C.R.; Cote, A.; Richards, B. Field Trials of the New DFIT-Flowback Analysis (DFIT-FBA) for Accelerated Estimates of Closure and Reservoir Pressure and Reservoir Productivity. In *Proceedings of the SPE/AAPG/SEG Unconventional Resources Technology Conference*; SPE: Richardson, TX, USA, 2020; p. D033S075R003.
85. Liu, G.; Ehlig-Economides, C. Comprehensive Model for the DFIT-Flowback Test Pumping, Shut-in, Choked Flowback, and Rebound Behavior. In *Proceedings of the 10th Unconventional Resources Technology Conference*; AAPG: Tulsa, OK, USA, 2022. [CrossRef]
86. Zeinabady, D.; Tabasinejad, F.; Clarkson, C.R. A stochastic method to optimize flowback DFIT ("DFIT-FBA") test design in tight reservoirs. *Gas Sci. Eng.* **2023**, *110*, 204874. [CrossRef]
87. Williams-Kovacs, J.D.; Deryushkin, D.; Hepburn, B.; Alexander, N. New Advancements in Flowback Analysis for Rapid Diagnostics and Integrated Hydraulic Fracture Optimization. In *Proceedings of the SPE Hydraulic Fracturing Technology Conference and Exhibition*; SPE: Richardson, TX, USA, 2024; p. D021S003R007.
88. Barree, R.D.; Miskimins, J.L.; Gilbert, J.V. Diagnostic fracture injection tests: Common mistakes, misfires, and misdiagnoses. *SPE Prod. Oper.* **2015**, *30*, 84–98. [CrossRef]

89. Hawkes, R.V.; Bachman, R.; Nicholson, K.; Cramer, D.D.; Chipperfield, S.T. Good Tests Cost Money, Bad Tests Cost More-A Critical Review of DFIT and Analysis Gone Wrong. In *Proceedings of the SPE International Hydraulic Fracturing Technology Conference and Exhibition*; SPE: Richardson, TX, USA, 2018; p. D013S004R001.
90. Zeinabady, D.; Zanganeh, B.; Shahamat, S.; Clarkson, C.R. Application of DFIT-FBA Tests Performed at Multiple Points in a Horizontal Well for Advanced Treatment Stage Design and Reservoir Characterization. In *Proceedings of the SPE Hydraulic Fracturing Technology Conference and Exhibition*; SPE: Richardson, TX, USA, 2021; p. D021S003R003.
91. Ibrahim Mohamed, M.; Ibrahim, A.F.; Ibrahim, M.; Pieprzica, C.; Ozkan, E. Determination of ISIP of Non-Ideal Behavior During Diagnostic Fracture Injection Tests. In *Proceedings of the SPE Annual Technical Conference and Exhibition?* SPE: Richardson, TX, USA, 2019; p. D022S088R002.
92. McClure, M.W.; Jung, H.; Cramer, D.D.; Sharma, M.M. The fracture-compliance method for picking closure pressure from diagnostic fracture-injection tests. *Spe J.* **2016**, *21*, 1321–1339. [CrossRef]
93. McClure, M.W.; Ratcliff, D.; Singh, A.; Ponners, C.; Fowler, G. *Practical Guidelines for DFIT Interpretation Using the 'Compliance Method' Procedure from URTeC-2019-123*; ResFrac Corporation: Austin, TX, USA, 2023.
94. Theis, C.V. The relation between the lowering of the piezometric surface and the rate and duration of discharge of a well using ground-water storage. *Eos Trans. Am. Geophys. Union* **1935**, *16*, 519–524. [CrossRef]
95. Jacob, C.E. Coefficients of storage and transmissibility obtained from pumping tests in the Houston district, Texas. *Eos Trans. Am. Geophys. Union* **1941**, *22*, 744–756. [CrossRef]
96. Gringarten, A.C. Type-curve analysis: What it can and cannot do. *J. Pet. Technol.* **1987**, *39*, 11–13. [CrossRef]
97. Abbaszadeh, M.; Asakawa, K.; Cinco-Ley, H.; Arihara, N. Interference testing in reservoirs with conductive faults or fractures. *SPE Reserv. Eval. Eng.* **2000**, *3*, 426–434. [CrossRef]
98. Martinez, N.R.; Samaniego, F.V. Advances in the analysis of pressure interference tests. *J. Can. Pet. Technol.* **2010**, *49*, 65–70. [CrossRef]
99. Chu, W.C.; Pandya, N.D.; Flumerfelt, R.W.; Chen, C. Rate-transient analysis based on the power-law behavior for permian wells. *SPE Reserv. Eval. Eng.* **2019**, *22*, 1360–1370. [CrossRef]
100. Chu, W.C.; Scott, K.D.; Flumerfelt, R.; Chen, C.; Zuber, M.D. A new technique for quantifying pressure interference in fractured horizontal shale wells. *SPE Reserv. Eval. Eng.* **2020**, *23*, 143–157. [CrossRef]
101. Almasoodi, M.; Andrews, T.; Johnston, C.; Singh, A.; McClure, M. A new method for interpreting well-to-well interference tests and quantifying the magnitude of production impact: Theory and applications in a multi-basin case study. *Geomech. Geophys. Geo-Energy Geo-Resour.* **2023**, *9*, 95. [CrossRef]
102. Ponners, C.; Babazadeh, M.; Cipolla, C.; Dhuldhoya, K.; Lu, Q.; Manchanda, R.; Tamayo, D.R.; Smith, S.; Shahri, M.; McClure, M. Interference testing in shale: A generalized 'Degree of Production Interference'(DPI) and developing new insights into the Chow Pressure Group (CPG). In Proceedings of the Unconventional Resources Technology Conference, Houston, TX, USA, 17–19 June 2024; pp. 2025–2052.
103. Awada, A.; Santo, M.; Lougheed, D.; Xu, D.; Virues, C. Is that interference? A work flow for identifying and analyzing communication through hydraulic fractures in a multiwell pad. *Spe J.* **2016**, *21*, 1554–1566. [CrossRef]
104. Gavrilov, A.V.; Togaev, S.E.; Limanskii, E.N.; Abidov, K.A. Well Interference Test in Naturally Fractured Gas Reservoir: Numerical Simulation and Impact on Reservoir Performance Forecasting. In *Proceedings of the SPE Annual Caspian Technical Conference*; SPE: Richardson, TX, USA, 2024; p. D011S003R003.
105. Liu, W.C.; Qiao, C.C.; Wang, P.; Huang, W.S.; Kong, X.W.; Sun, Y.P.; Sun, H.D.; Jia, Y.P. Study of interwell interference in shale gas reservoirs by a robust production data analysis method based on deconvolution. *Pet. Sci.* **2024**, *21*, 2502–2519. [CrossRef]
106. Cooke, C.E., Jr. Method of Determining Fluid Saturations in Reservoirs. 1971. Available online: https://www.osti.gov/biblio/5557028 (accessed on 30 May 2025).
107. Tomich, J.F.; Dalton, R.L.; Deans, H.A.; Shallenberger, L.K. Single-Well Tracer Method To Measure Residual Oil Saturation. *J. Pet. Technol.* **1973**, *25*, 211–218. [CrossRef]
108. Asakawa, K. Numerical Modeling and Simulations of Microbial Enhanced Oil Recovery and Tracer Tests. Ph.D. Thesis, The University of Texas at Austin, Austin, TX, USA, 2005.
109. Jin, M.; Delshad, M.; Dwarakanath, V.; McKinney, D.C.; Pope, G.A.; Sepehrnoori, K.; Tilburg, C.E.; Jackson, R.E. Partitioning Tracer Test for Detection, Estimation, and Remediation Performance Assessment of Subsurface Non aqueous Phase Liquid. *Water Resour. Res.* **1995**, *31*, 1201–1211. [CrossRef]
110. McGuire, P.L.; Chatham, J.R.; Paskvan, F.K.; Sommer, D.M.; Carini, F.H. Low salinity oil recovery: An exciting new EOR opportunity for Alaska's North Slope. In *SPE Western Regional Meeting*; SPE: Richardson, TX, USA, 2005; p. SPE-93903.
111. Behrens, H.; Beims, U.; Dieter, H.; Dietze, G.; Eikmann, T.; Grummt, T.; Hanisch, H.; Henseling, H.; Käß, W.; Kerndorff, H.; et al. Toxicological and ecotoxicological assessment of water tracers. *Hydrogeol. J.* **2001**, *9*, 321–325. [CrossRef]
112. Becker, M.W.; Coplen, T.B. Use of deuterated water as a conservative artificial groundwater tracer. *Hydrogeol. J.* **2001**, *9*, 512–516. [CrossRef]

113. Shook, G.M.; Pope, G.A.; Asakawa, K. Determining reservoir properties and flood performance from tracer test analysis. In *Proceedings of the SPE Annual Technical Conference and Exhibition?* SPE: Richardson, TX, USA, 2009; p. SPE-124614.
114. Li, H.; Liu, Z.; Li, Y.; Luo, H.; Cui, X.; Nie, S.; Ye, K. Evaluation of the release mechanism of sustained-release tracers and its application in horizontal well inflow profile monitoring. *ACS Omega* **2021**, *6*, 19269–19280. [CrossRef] [PubMed]
115. Gombert, P.; Biaudet, H.; Sèze, R.; de Pandard, P.; Carré, J. Toxicity of fluorescent tracers their degradation byproducts. *Int. J. Speleol.* **2017**, *46*, 5. [CrossRef]
116. Du, Y.; Guan, L. Interwell tracer tests: Lessons learned from past field studies. In *Proceedings of the SPE Asia Pacific Oil and Gas Conference and Exhibition*; SPE: Richardson, TX, USA, 2005; p. SPE-93140.
117. King, G.E.; Leonard, D. Utilizing fluid and proppant tracer results to analyze multi-fractured well flow back in shales: A framework for optimizing fracture design and application. In *Proceedings of the SPE Hydraulic Fracturing Technology Conference and Exhibition*; SPE: Richardson, TX, USA, 2011; p. SPE-140105.
118. Tian, W.; Shen, T.; Liu, J.; Wu, X. Hydraulic fracture diagnosis using partitioning tracer in shale gas reservoir. In *Proceedings of the SPE Asia Pacific Hydraulic Fracturing Conference*; SPE: Richardson, TX, USA, 2016; p. D022S010R039.
119. Liu, J.; Jiang, L.; Liu, T.; Yang, D. Field-Scale Modeling of Interwell Tracer Flow Behavior to Characterize Complex Fracture Networks Based on the Embedded Discrete Fracture Model in a Naturally Fractured Reservoir. *SPE J.* **2023**, *28*, 1062–1082. [CrossRef]
120. Albrecht, M.; Borchardt, S.; Murphree, C.; McClure, M.; Rondon, J. Using quantitative tracer analysis to calibrate hydraulic fracture and reservoir simulation models: A Permian Basin case study. In *Proceedings of the SPE/AAPG/SEG Unconventional Resources Technology Conference*; SPE: Richardson, TX, USA, 2022; p. D021S031R003.
121. Jain, L.; Cooper, J.; Singh, A. Novel tracer application and analysis methodology to quantify creation and drainage of hydraulic fracture area and growth rate. In Proceedings of the Unconventional Resources Technology Conference, Houston, TX, USA, 17–19 June 2024; pp. 959–974.
122. Yang, H.; Guo, K.; Lin, L.; Zhang, S.; Wang, Y. Application of micro-substance tracer test in fractured horizontal wells. *J. Pet. Explor. Prod. Technol.* **2024**, *14*, 1235–1246. [CrossRef]
123. Rose, P.E.; Jones, C.; Simmons, S.; McLennan, J.; England, K. Tracer Testing in Well 16B-32 at the Utah FORGE EGS Project. In *Proceedings of the 49th Workshop on Geothermal Reservoir Engineering (Stanford Geothermal Workshop)*; Stanford University: Stanford, CA, USA, 2024.
124. Chen, Y.C.; Jolicoeur, B.; Chueh, C.C.; Wu, K.T. Flow coupling between active and passive fluids across water–oil interfaces. *Sci. Rep.* **2021**, *11*, 13965. [CrossRef] [PubMed]
125. Ding, M.; Yuan, F.; Wang, Y.; Xia, X.; Chen, W.; Liu, D. Oil recovery from a CO_2 injection in heterogeneous reservoirs: The influence of permeability heterogeneity, CO_2-oil miscibility and injection pattern. *J. Nat. Gas Sci. Eng.* **2017**, *44*, 140–149. [CrossRef]
126. Ghergut, I.; Behrens, H.; Sauter, M. Tracer-based quantification of individual frac discharge in single-well multiple-frac backflow: Sensitivity study. *Energy Procedia* **2014**, *59*, 235–242. [CrossRef]
127. Kumar, A.; Sharma, M.M. Diagnosing fracture-wellbore connectivity using chemical tracer flowback data. In *Proceedings of the SPE/AAPG/SEG Unconventional Resources Technology Conference*; SPE: Richardson, TX, USA, 2018; p. D013S015R007.
128. Liu, J.; Jiang, L.; Liu, T.; Yang, D. Modeling tracer flowback behaviour for a multifractured horizontal well in a tight oil reservoir using the embedded discrete fracture model. *J. Pet. Sci. Eng.* **2022**, *212*, 110347. [CrossRef]
129. Du, D.; Hao, F.; Li, Y.; Li, D.; Tang, Y. Study on Interpretation Method of Multistage Fracture Tracer Flowback Curve in Tight Oil Reservoirs. *ACS Omega* **2024**, *9*, 11628–11636. [CrossRef] [PubMed]
130. Tian, W.; Darnley, A.; Mohle, T.; Johns, K.; Dempsey, C. Understanding frac fluid distribution of an individual frac stage from chemical tracer flowback data. In *Proceedings of the SPE Hydraulic Fracturing Technology Conference and Exhibition*; SPE: Richardson, TX, USA, 2019; p. D022S005R002.
131. Arshad, W.; Brohi, I.; Pooniwala, S. Changing the Status Quo: First Application of Utilizing Novel Tracer Technology for Monitoring Hydraulic Fracture Stage Contribution. In Proceedings of the International Petroleum Technology Conference; IPTC: Richardson, TX, USA, 2024; p. D011S015R007.
132. Asadi, M.; Blair, T.; Ryan, J. DNA Tracer Application in a Waterflood Study in Edmisson Field: A Case History. In *Proceedings of the SPE Annual Technical Conference and Exhibition?* SPE: Richardson, TX, USA, 2013; p. D012S002R003.
133. Ren, M.; Yang, B.; Yang, D.; Liu, Y.; Zhang, H.; Zhang, M.; Zhang, Y. Optimizing the preparation of multi-colored dye-tracer proppants: A potential approach for quantitative localization and volume assessment of proppant flowback in multistage fractured horizontal wells. *Geoenergy Sci. Eng.* **2024**, *240*, 213053. [CrossRef]
134. El Khouly, I.; Sabet, A.; El-Fattah, M.A.; Bulatnikov, M. Integration Between Different Hydraulic Fracturing Techniques and Machine Learning in Optimizing and Evaluating Hydraulic Fracturing Treatment. In *Proceedings of the International Petroleum Technology Conference*; IPTC: Richardson, TX, USA, 2024; p. D021S084R003.
135. Alsiyabi, K.; Al-Aamri, M.H.; Kazemi, A.; Nejad, G. Wavelet Transform for Fracture Diagnostics in Tight Gas Sandstone. In *Proceedings of the SPE EOR Conference at Oil and Gas West Asia*; SPE: Richardson, TX, USA, 2025; p. D011S005R006.

136. Soliman, M.Y.; Ansah, J.; Stephenson, S.; Mandal, B. Application of wavelet transform to the analysis of pressure-transient data. *SPE Reserv. Eval. Eng.* **2003**, *6*, 89–99. [CrossRef]
137. Gabry, M.A.; Ramadan, A.; Soliman, M.Y. Advanced Fracture Diagnostics in Utah FORGE Enhanced Geothermal Systems (EGS): Integrating Continuous Wavelet Transform (CWT), Microseismic, and Fiber-Optic Data for Enhanced Stimulation Insights. In *Proceedings of the SPE Annual Technical Conference and Exhibition*; SPE: Richardson, TX, USA, 2024; p. D031S031R002.
138. Liu, X.; Chen, Z.; Zhang, X.D.; Zhong, G.Y.; Li, S.M. An efficient hydraulic fracturing fracture network connectivity evaluation method based on point cloud pattern recognition. In *ARMA US Rock Mechanics/Geomechanics Symposium*; ARMA: Houston, TX, USA, 2024; p. D042S062R007.
139. Chen, Z.; Jiang, X.; Pan, Z.; Jeffrey, R.G. Coupled inversion of pressure and tiltmeter data for mapping hydraulic fracture geometry. *Acta Mech. Solida Sin.* **2024**, *37*, 396–405. [CrossRef]
140. Salimzadeh, S.; Kasperczyk, D.; Sayyafzadeh, M.; Kadeethum, T. Inferring fracture dilation and shear slip from surface deformation utilising trained surrogate models. *Int. J. Rock Mech. Min. Sci.* **2025**, *188*, 106077. [CrossRef]
141. Akbari, A.; Karami, A.; Kazemzadeh, Y.; Ranjbar, A. Evaluation of hydraulic fracturing using machine learning. *Sci. Rep.* **2025**, *15*, 26926. [CrossRef]
142. Ma, Y.; Ye, M. Application of machine learning in hydraulic fracturing: A review. *ACS Omega* **2025**, *10*, 10769–10785. [CrossRef]
143. Khan, A.M.; Ugarte, E.; Kurniadi, S.; Al Shueili, A.; Wang, W.K. Physics-Informed Machine Learning for Hydraulic Fracturing—Part III: The Transfer Learning Validation. In *Proceedings of the International Petroleum Technology Conference*; IPTC: Richardson, TX, USA, 2025; p. D022S005R007.
144. Pan, Z.; Zhu, L.; Xue, Y.; Xu, H. Fluid Flow in Fractured Rocks: From Multiphysics Paradigms to AI-Driven Predictive Modeling. *Fluid Dyn. Mater. Process.* **2026**, *22*, 2. [CrossRef]
145. Yao, J.; Li, X.; Xiang, J. Design of a hybrid model of finite element method and machine learning to predict mode I–II crack expansions. In *Proceedings of the SPIE—International Society for Optical Engineering*; Yang, S.X., Karras, D.A., Eds.; SPIE: Bellingham, WA, USA, 2023.
146. Zhou, X.; He, S.; Dong, L.; Atluri, S.N. Real-time prediction of probabilistic crack growth with a helicopter component digital twin. *AIAA J.* **2022**, *60*, 2555–2567. [CrossRef]
147. Niu, S.; Srivastava, V. Simulation trained CNN for accurate embedded crack length, location, and orientation prediction from ultrasound measurements. *Int. J. Solids Struct.* **2022**, *242*, 111521. [CrossRef]
148. Wang, Z.; Li, J.; Liu, X.; Zhang, S.; Lin, Y.; Tan, J. Diameter-adjustable mandrel for thin-wall tube bending and its domain knowledge-integrated optimization design framework. *Eng. Appl. Artif. Intell.* **2025**, *139*, 109634. [CrossRef]
149. Wan, M.; Pan, Y.; Zhang, Z. A Physics-Informed Neural Network Integration Framework for Efficient Dynamic Fracture Simulation in an Explicit Algorithm. *Appl. Sci.* **2025**, *15*, 10336. [CrossRef]
150. Ryu, Y.; Shah, P.; Na, J.; Kwon, J.S.I. Physics-informed neural network with moving boundary constraints for modeling hydraulic fracturing. *Comput. Chem. Eng.* **2025**, *203*, 109308. [CrossRef]
151. Chen, J.; Yu, H.; Li, B.; Zhang, H.; Jin, X.; Meng, S.; Liu, H.; Wu, H. DeepONet-embedded physics-informed neural network for production prediction of multiscale shale matrix–fracture system. *Phys. Fluids* **2025**, *37*, 016608. [CrossRef]
152. Abdelghany Elkotb, M.; Naveed Khan, M.; Ali, A.B.M.; Kumar, A.; Alwan, S.H.; Alrihieli, H.F. Machine learning-augmented finite element modeling for fracture mechanics: A systematic review and future research directions. *SSRN Electron. J.* **2025**. [CrossRef]

Disclaimer/Publisher's Note: The statements, opinions and data contained in all publications are solely those of the individual author(s) and contributor(s) and not of MDPI and/or the editor(s). MDPI and/or the editor(s) disclaim responsibility for any injury to people or property resulting from any ideas, methods, instructions or products referred to in the content.